

國立交通大學

電子工程學系電子研究所



研究生：黃國隆

指導教授：杭學鳴博士

中華民國九十八年五月

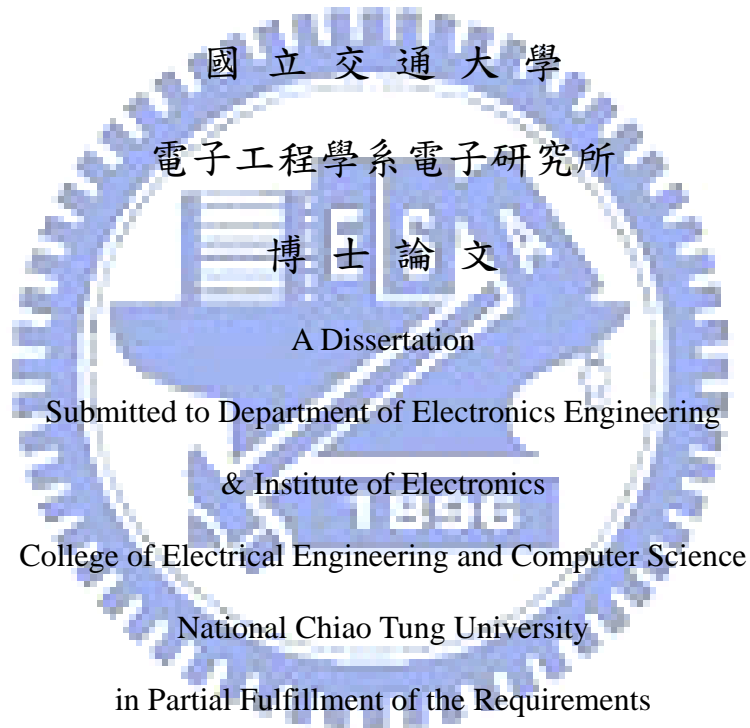
用於相依視訊編碼之影質控制策略  
Picture Quality Control Strategies for  
Dependent Video Coding

研究生：黃國隆

Student : Kao-Lung Huang

指導教授：杭學鳴博士

Advisor : Dr. Hsueh-Ming Hang



for the Degree of

Doctor of Philosophy

in

Electronics Engineering

May 2009

Hsinchu, Taiwan, Republic of China

中華民國九十八年五月

# 用於相依視訊訊編碼 之影質控制策略

研究生：黃國隆

指導教授：杭學鳴 博士

國立交通大學 電子工程學系 電子研究所博士班

## 摘要

傳統視訊位元率控制演算法通常追求影像失真總量最小化，然而往往付出影值大幅度變動的代價，特別是在視訊內容較激烈且經常性場景變換時。為了減輕影值變動所帶來的負面作用，許多演算法追求全部影值均等。如某些研究者指出，雖然現有演算法已能產生影值均等的視訊，但是這些演算法經常無法精確地使用分配的位元來減少失真總量。本論文嘗試一次達成三個目標。即平穩視訊品質、失真總量最小化、精準地使用位元預算等。我們共提供三個演算法，針對兩種不同應用，定速率與變速率通道，來完成這些目標。其中兩個演算法適用於定速率通道，如儲存應用；一個演算法適用於變速率通道，如網際網路傳輸應用。

第一個演算法使用籬柵圖(Trellis-Based)架構來達成具備一致性品質的視訊。我們第一個貢獻是推導出，失真最小化問題與位元預算最小化問題的等效條件。第二，籬柵圖狀態定義為失真量，方便於一致性品質控制。第三，只需在提出的演算法中調整一個參數，一個介於，最小失真總量與固定品質的視訊解，可以被求得。第二個演算法結合拉格蘭乘數(Lagrange Multiplier)、快速分支延展與最佳化程序。與第一個演算法比較，

它的峰信雜比效能只有些微的降低，但是運算複雜度顯著地降低。模擬結果顯示，這兩個演算法都只比 MPEG 所提 JM 位元率控制演算法的平均峰信雜比些微低。當與近期發表的 MultiStage 與 LPF 演算法比較，我們所提演算法能夠較準確地使用分配位元預算，且輸出最大的峰信雜比與很小的峰信雜比變動率。

第三個演算法在變速率通道追求優雅的品質變動。我們取代一致性品質限制，換成最大相鄰幀間影值變動限制。因為這個演算法在單獨 GOP 內運作，相鄰 GOP 品質控制需求也需要被考量。每個 GOP 通道位元率被設定成給定的頻寬晃動模型。模擬結果顯示，我們的峰信雜比曲線函數很平滑，且在每個 GOP 邊界並沒有品質突然掉落。我們所提演算法也能夠準確地利用分配位元預算值。

總結，我們發展出彈性的影值控制架構，提出三個演算法。這些解能滿足三個目標，品質變動最小化、失真總量最小化、精準地使用位元預算。此外，附錄 A 呈現通道編碼效能分析結果，未來可用於整合視訊與通道編碼研究。



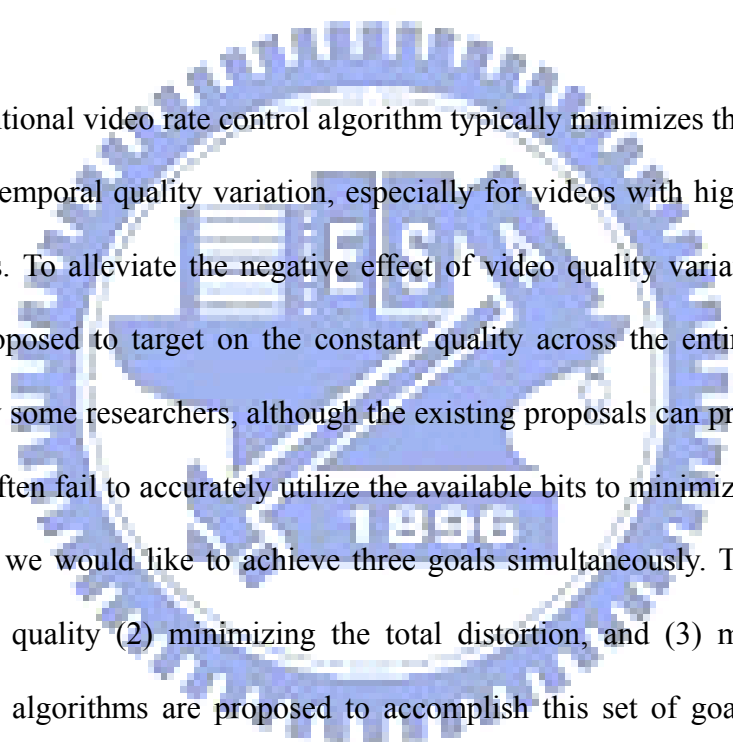
# Picture Quality Control Strategies for Dependent Video Coding

Student: Kao-Lung Huang

Advisor: Dr. Hsueh-Ming Hang

Department of Electronics Engineering and Institute of Electronics  
National Chiao Tung University

## ABSTRACT



A conventional video rate control algorithm typically minimizes the total distortion at the cost of large temporal quality variation, especially for videos with high motion and frequent scene changes. To alleviate the negative effect of video quality variation, a few algorithms have been proposed to target on the constant quality across the entire sequence. As being pointed out by some researchers, although the existing proposals can produce constant-quality videos, they often fail to accurately utilize the available bits to minimize the global distortion. In this thesis, we would like to achieve three goals simultaneously. They are (1) producing smooth video quality (2) minimizing the total distortion, and (3) meeting the bit budget strictly. Three algorithms are proposed to accomplish this set of goals for two application scenarios: constant bitrate channels and variable bitrate channels. Two algorithms are designed for the constant bitrate channels, which may be used on the storage applications. And one algorithm is designed for the variable bitrate channels, which is needed for, say, Internet transmission applications.

The first algorithm uses the trellis-based structure to achieve the consistent quality video. Our first contribution is to derive an equivalent condition between the distortion minimization problem and the budget minimization problem. Second, the trellis state (tree node) is defined in terms of distortion, which facilitates the consistent quality control. Third, by adjusting one

key parameter in our algorithm, a solution in between the minimum total distortion and the constant quality criteria can be obtained. The second algorithm combines the Lagrange multipliers together with the proposed fast branch expansion process and optimization procedure. Compared to the first algorithm, its PSNR performance is degraded slightly but the computational complexity is significantly reduced. Simulation results show that our two algorithms produce a much smaller PSNR variation at a slight average PSNR loss as compared to the MPEG committee JM rate control. When they are compared to the recently published MultiStage and LPF algorithms, our proposed algorithms can meet the bit budget more accurately and produce the largest average PSNR at a small PSNR variation.

The third algorithm aims at graceful quality variation for time-varying channels. We replace the consistent quality constraint in the second algorithm by a maximal inter-frame quality variation constraint. Because this algorithm operates on individual GOP's, the quality variation across GOP boundaries has also to be considered. In our experiments, the channel bit rate for each GOP is set to follow the given bandwidth fluctuation pattern. Simulation results show that our PSNR curve has a smoother shape and has no sudden drop at the GOP boundaries. Also, the proposed algorithm meets the budget bits very accurately.

In summary, we develop a flexible quality control framework that leads to 3 separate algorithms. They are nearly optimal solutions that achieve the triple goal: minimizing quality variation, minimizing global distortion, and satisfying the bit budget constraint. In addition, a channel coding study is presented in Appendix A for solving combined source-channel coding in the future.

# 誌 謝

能完成論文，首先要感謝杭學鳴老師多年來的悉心指導。杭老師不僅在做研究上給予指導與鼓勵，同時也關心工作上所遇困難，尤其感謝杭老師在論文發表過程，持續不斷的鼓勵與指導，讓我學到更多為人處事的道理。

感謝通訊電子與訊號處理實驗室諸位學長、同學、學弟妹的互相鼓勵、研究討論，使我得以在相關知識上有所增長。尤其要謝謝峰誠、郁男這些年來在研究及生活上的幫忙。也感謝每一位曾教導過我的老師與系上歷任助理在行政事務上的協助，還有中科院長官們提名拔擢，讓我有此難得的進修機會。

最後，我要致上最深的感謝給我的父母、我的太太瑞鴛、我的孩子丞廷與丞鈞，你們的支持是我最大的精神支柱，讓我能專心完成學業。願與你們一同分享這份喜悅。



~ in memory of my father ~



# 目 錄

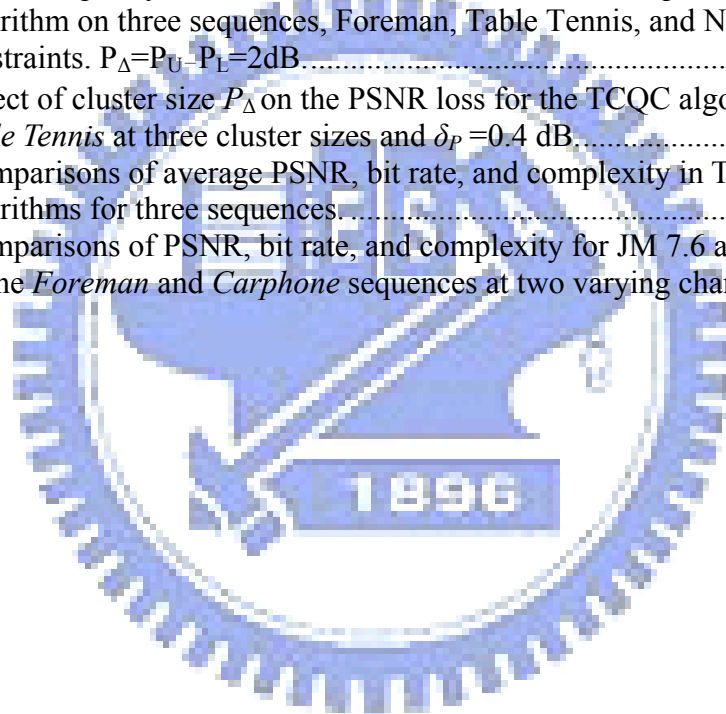
摘 要 .....	i
ABSTRACT .....	iii
誌 謝 .....	v
目 錄 .....	vii
List of Tables .....	ix
List of Figures.....	x
Chapter 1 Introduction.....	1
1.1 Motivation and Discussed Topics.....	1
1.2 Organization of the Thesis.....	3
1.3 Contributions of the Thesis.....	4
Chapter 2 Overview of Lossy Video Coding.....	5
2.1 Dependent and Independent Video Coding.....	5
2.2 Rate-Distortion bound and Optimality.....	6
2.3 Rate-Distortion Optimization Criteria.....	8
2.4 Trellis Representation of the Tree Structure.....	9
2.5 Rate-Distortion Optimization Techniques.....	10
2.5.1 Lagrange Multiplier.....	10
2.5.2 Lagrange Relaxation.....	11
2.5.3 Dynamic Programming.....	12
2.6 Joint Source-Channel Coding.....	13
Chapter 3 Consistent Quality Control Algorithms.....	14
3.1 Problem Formulation and Distortion-Rate Function.....	14
3.1.1 Dependent MINAVE Bit Allocation Problem.....	14
3.1.2 Uniqueness of Distortion-Rate Function.....	16
3.2 Consistent Quality Control Algorithm.....	17
3.2.1 Trellis-Based Coding Scheme.....	17
3.2.2 Branch Expansion and Frame-level Bit Allocation.....	19
3.2.3 Fast Branch Expansion Process.....	21
3.2.4 Technique based on the Lagrange Multipliers.....	22
3.3 Simulation Results.....	25
3.3.1 Performance Comparison with Constant QP and JM.....	26
3.3.2 LCQC Performance Comparison with LPF and MultiStage Algorithms.....	30
3.3.3 Effects of Quality Variation Constraint on PSNR and Complexity.....	34
3.3.4 Effects of Cluster Size on PSNR and Complexity.....	37
3.4 Summary.....	38
Chapter 4 Graceful Quality Control Algorithm.....	40
4.1 Graceful Quality Variation Problem.....	40
4.2 Graceful Quality Control Algorithm.....	41
4.3 Simulation Results.....	43
4.3.1 LGQC Performance Comparison with JM.....	44
4.3.2 Effects of Quality Variation Constraint on PSNR and Complexity.....	47
4.4 Summary.....	50
Chapter 5 Conclusions and Future Research Topics.....	52
Appendix A Performance Analysis for Serially Concatenated FEC in IEEE802.16a over	

Wireless Channels .....	54
A.1 Introduction .....	54
A.2 System Mode .....	55
A.3 Performance of Serially Concatenated FEC .....	57
A.3.1 Union Upper Bound on the BER of RCPC Codes .....	57
A.3.2 Union Upper Bound on BER of RS Codes.....	58
A.4 Simulation Results .....	58
A.5 Conclusions .....	62



# List of Tables

Table 3.1. Comparisons of Minimum PSNR, Maximum PSNR, Average PSNR, PSNR Variance, Bit Rate, and Decoding Delay for JM 7.6, TCQC, and Constant QP Schemes on the Foreman Sequence.....	27
Table 3.2. Comparisons of Minimum PSNR, Maximum PSNR, Average PSNR, PSNR Variance, Bit Rate, and Decoding Delay for JM 7.6, TCQC, and Constant QP Schemes on the News Sequence.....	27
Table 3.3. Comparisons of PSNR, bit rate, and complexity for LCQC, MultiStage, and LPF algorithms on <i>News</i> at three bit rates.....	34
Table 3.4. Comparisons of PSNR, bit rate, and complexity for LCQC, MultiStage, and LPF algorithms on <i>Table Tennis</i> at three bit rates. ....	34
Table 3.5. Effect of quality variation constraint on PSNR and complexity for the LCQC algorithm on three sequences, Foreman, <i>Table Tennis</i> , and <i>News</i> at three quality constraints. $P_{\Delta}=P_U-P_L=2\text{dB}$ .....	35
Table 3.6. Effect of cluster size $P_{\Delta}$ on the PSNR loss for the TCQC algorithm on <i>Foreman</i> and <i>Table Tennis</i> at three cluster sizes and $\delta_p=0.4\text{ dB}$ .....	38
Table 3.7. Comparisons of average PSNR, bit rate, and complexity in TCQC and LCQC algorithms for three sequences.....	38
Table 4.1. Comparisons of PSNR, bit rate, and complexity for JM 7.6 and LGQC algorithms on the <i>Foreman</i> and <i>Carphone</i> sequences at two varying channel bit rates. ....	47



# List of Figures

Fig.2.1. An illustration of hybrid motion compensated video Encoder.....	6
Fig.2.2. An illustration of Operational R-D Characteristic. ....	7
Fig.2.3. Comparison of frame 248 coding results on the Carphone sequence between MINMAX.....	9
Fig.3.1. An illustration of cluster, node, branch, $P_{\Delta}$ , and $\delta_p$ definitions.....	19
Fig.3.2. PSNR and used bit plots of the TCQC, JM 7.6, and Constant QP algorithms for <i>News</i> at two bit rates. (a) PSNR plots at 24 kbps (b) Used bit plots at 24 kbps (c) PSNR plots at 112 kbps (d) Used bit plots at 112 kbps.....	30
Fig.3.3. PSNR and used bit plots of the LCQC, MultiStage, and LPRF algorithms $P_{\Delta} = 2.0$ dB and $\delta_p = 0.2$ dB at 64 kbps: (a) PSNR plots for <i>News</i> (b) Used bit plots for <i>News</i> (c) PSNR plots for <i>Table Tennis</i> (d) Used bit plots for <i>Table Tennis</i> . ....	33
Fig.3.4. LCQC results for <i>News</i> at 24 kbps and $P_{\Delta}=2.0$ dB : (a) $\delta_p = 0.2$ dB. (b) $\delta_p = 0.4$ dB.(c) $\delta_p = 1.0$ dB.....	37
Fig.4.1. Channel bit rate patterns for LGQC graceful quality control test on two different video sequences. (a) <i>Foreman</i> , and (b) <i>Carphone</i> .....	45
Fig.4.2. PSNR plots of the LGQC and JM7.6 algorithms for two sequences at two different channel bit rates. (a) Foreman sequence using rate pattern in Fig. 4.1(a). (b) Carphone sequence using rate pattern in at Fig. 4.1(b).....	47
Fig.4.3. PSNR and used bit plots of the LGQC with two $\delta_p$ values and JM7.6 algorithms for two sequences at two different channel bit rates. (a) Foreman sequence PSNR plots at Fig. 4.1(a) bit rate. (b) Foreman sequence used bit plots at Fig. 4.1(a) bit rate. (c) Carphone sequence PSNR plots at Fig. 4.1(b) bit rate. (d) Carphone sequence used bit plots at Fig. 4.1(b) bit rate. ....	50
Fig.A.1. System model. ....	56
Fig.A.2. BER of RCPC codes in AWGN. ....	59
Fig.A.3. BER of RCPC codes in FI RFC. ....	60
Fig.A.4. BER of RS code in AWGN. ....	60
Fig.A.5. BER of RS code in FI-RFC.....	61
Fig.A.6. PER of RS code in AWGN.....	61
Fig.A.7. PER of RS code in FI-RFC. ....	62

# Chapter 1

## Introduction

Video coding technologies have been progressing very fast in the past two decades. International video coding standards such as MPEG-1 [1], MPEG-2 [2], MPEG-4 [3], H.263 [4], and H.264/AVC [5-7] are developed to achieve efficient transmission and storage in various environments. These coding standards specify the decoding process and the bit-stream syntax only. This limitation of scope permits maximal freedom to optimize the encoder for coding performance improvement and complexity reduction.

### 1.1 Motivation and Discussed Topics

Due to the motion estimator and other inter-frame operations, the standard-compliant video coding is an inherently *dependent coding* process [8-11]. To achieve the optimal rate-distortion (R-D) performance, *rate control* algorithms are usually applied to fulfill some optimization criteria [12-17]. There are two commonly used optimization criteria: minimum average distortion (the MINAVE criterion) and minimum maximum distortion (the MINMAX criterion) [18]. This MINAVE criterion is widely adopted and is well studied in the literature [19-22]. However, this MINAVE goal is attained often at the expense of a possibly larger frame-by-frame quality variation. From the perspective of human visual system (HVS), a video sequence with nearly constant quality or *consistent quality* is more desirable. Therefore, the MINMAX criterion is proposed to minimize the maximal distortion for a given bit budget [23-27]. Often, the MINMAX results do not achieve strictly the global MINMAX target. They typically produce videos with a slowly varying quality, or in other words, with a consistent quality, and this is practically all we need. However, the MINMAX criterion decreases the

frame-by-frame quality variation without paying attention to the total distortion. Therefore, a hybrid MINMAX/MINAVE method [28] was suggested to increase the overall quality after finding the MINMAX solution.

In this thesis, we first tackle the dependent MINAVE and consistent-quality problems simultaneously for the storage applications. More specifically, we would like to achieve the consistent quality goal across the entire sequence and, in the meantime, to meet the target bit rate accurately and to minimize the total distortion. The trade-off between average distortion and consistent quality is controlled by one key parameter, namely, the maximal quality variation constraint. One method to solve the above optimization problem with finite parameter set is the dynamic programming approach [12, 18]. By adopting the monotonicity and clustering concepts [9], the tree structure in the *dependent video coding* is converted into a trellis diagram [11]. Thus, the Viterbi algorithm [29] can be employed to find the truly optimal solution in this dependent coding problem. The trellis state (tree node) is defined in terms of distortion to facilitate the consistent quality control. In addition, a fast technique is proposed to decrease the computation in the branch expansion process. By adjusting the key parameters in our scheme such as cluster size, we can decrease the computational complexity at the cost of minor performance loss. A second method is proposed based on the Lagrange multipliers [12]. To ensure the global optimality on the dependent coding platform, an iterative scheme is designed to find the best lambda ( $\lambda$ ) parameter (Lagrange multiplier) in the Lagrange cost or Lagrangian. This algorithm backtracks many times to narrow down a valid  $\lambda$  range containing the optimal  $\lambda$ . Then, the best  $\lambda$  value is identified by a fast search algorithm [30]. This scheme runs much faster than the trellis-based approach. Its performance is close to but slight lower than that of the trellis-based approach.

Next we would like to show that the proposed scheme has the capability of graceful quality variation on the time-varying channel. The time-varying channel is equivalently

represented by the time-varying GOP bit budget. The graceful quality fluctuation across the GOP boundary is achieved by constraining the distortion variation of the first frame in one GOP with respect to its previous frame. Under this cross-GOP constraint, we can achieve the graceful quality fluctuation goal across the entire sequence while minimizing the total distortion and meeting the bit budget accurately in a GOP.

Despite the optimality of both methods suggested in this thesis, their real-time implementation is still beyond the current hardware capability. Thus, the proposed algorithms may be more suitable for off-line applications such as DVD playback when video quality is the major concern. We implement our algorithm on the new and very efficient H.264 coder and evaluate its performance.

## 1.2 Organization of the Thesis

The rate-distortion issues in lossy and dependent video coding problem are described in Chapter 2. We then develop effective algorithms to achieve three goals simultaneously: (a) producing consistent quality videos, (b) minimizing the total distortion and (c) meeting the bit budget strictly in Chapter 3. A mathematical proposition is derived to set up its theoretical foundation. Two new algorithms are proposed to accomplish this goal. One is the trellis-based algorithm with Viterbi search and the other one is the Lagrangian-based iterative algorithm with bisection search. Moreover, the proposed algorithms can produce a solution in between the MINAVE and the constant quality extremes. Extensive simulations are conducted to verify these goals.

Chapter 4 targets on the smooth video representation for time-varying channels. We wish to both minimize the total distortion and meet the bit budget accurately. The third algorithm is thus proposed to solve this problem. The detailed procedures are described and verified by simulation over a time-varying channel. Experimental results show that the proposed

algorithm can accommodate the time-varying channel bandwidth and its PSNR performs in a “graceful degradation” way.

Finally, Chapter 5 summarizes the findings in this thesis and the research topics in the future. Appendix A presents the performance analysis on the serially concatenated forward error correction (FEC) scheme in IEEE802.16a over the wireless channels. We study this channel coding topic for the future joint source-channel research.

## 1.3 Contributions of the Thesis

The main contributions of this thesis are:

1. We derive a theoretical proposition where an equivalent condition between the distortion minimization problem and the budget minimization problem is proposed. This proposition is the theoretical basis of our quality control algorithms.
2. We show that the triple goal of consistent quality video, total distortion minimization, and meeting the bit budget strictly can be achieved simultaneously by the trellis-based dependent coding structure.
3. By adjusting one key parameter, the proposed framework can achieve a solution in between the MINAVE and the constant quality criteria.
4. We propose a Lagrange-based algorithm together with the fast branch expansion technique to significantly reduce the computational complexity in the trellis-based framework. The resulting PSNR performance is close to that of the trellis one except for a slight average PSNR loss.
5. Targeting at the time-varying channels with bandwidth fluctuation, a modified Lagrange-based algorithm is proposed. It is able to follow the channel bitrate changes and produce a smooth video representation and minimize the total distortion.



# Chapter 2

## Overview of Lossy Video Coding

A compromise between the rate and the distortion is an inherent nature of every lossy compression scheme. In this chapter, we describe the basic knowledge related to R-D methods. Rate and distortion are measured in bit and mean squared error (MSE) respectively. Video coding property, R-D performance bound, two R-D optimization criteria, and three R-D optimization techniques are introduced to build up the foundation of this thesis.

### 2.1 Dependent and Independent Video Coding

The hybrid motion compensated video coding standards as shown in Fig. 2.1 exploit spatial and temporal redundancy through transform coding and motion estimation. Due to the motion estimator and the other inter-frame operations in standard-compliant coding framework, it results in the so-called *dependent coding* structure. In the dependent coding, a tree structure is usually adopted to represent all possible picture sequences.

Mathematically, the exhaustive search for the optimal frame QPs in a group of pictures (GOP) is equivalent to finding the optimal path in a tree. Potentially, this approach can identify the globally optimal solution. However, the computational complexity grows exponentially as more pictures are coded. For optimal rate-distortion (R-D) solution, several methods are proposed to reduce the search complexity, for example, the monotonicity assumption [9], the node clustering [11], the steepest descent search [10] and the inter-frame R-D model [17].

A sub-optimal approach simplifies the original structure by adopting the *independent coding* assumption [12], which picks up the best parameters for the current frame without

considering their effects on the future frames. Many practical *one-pass* or *two-pass* algorithms belong to this category and they include R-D models such as the classical statistical model [13-14], the quadratic model [15], and the rho-domain model [16]. The R-D optimality is not guaranteed in this approach because of the unavailability of future frames.

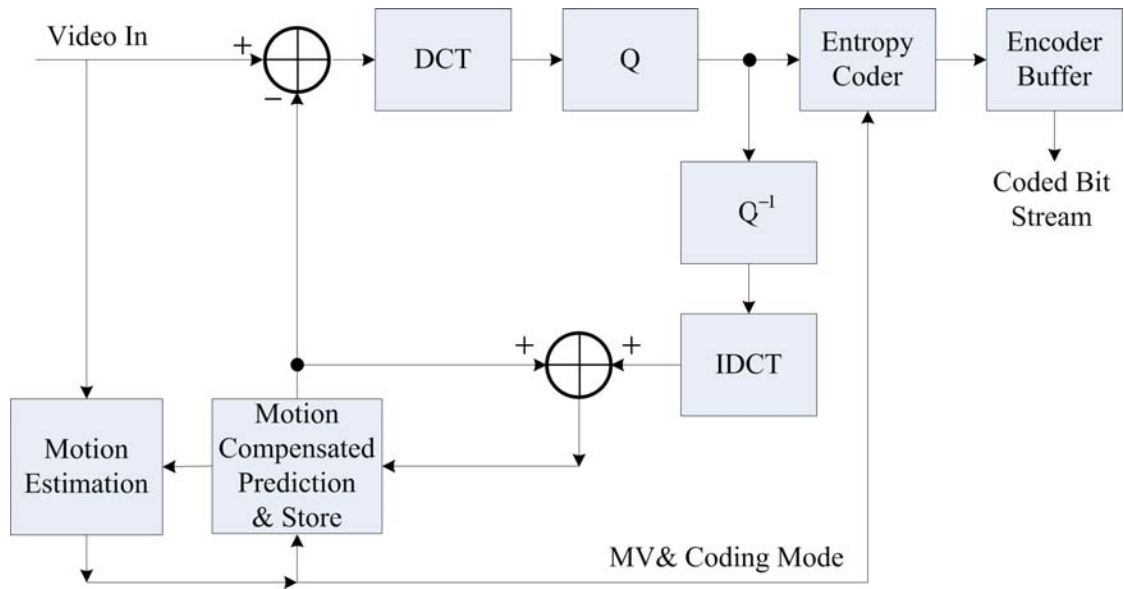


Fig.2.1. An illustration of hybrid motion compensated video Encoder.

## 2.2 Rate-Distortion bound and Optimality

R-D theory has been actively studied in the information-theory community for the last 60 years [31-33]. These studies focus on the derivation of performance bounds where the region of achievable points in the R-D trade-off is determined for certain statistical source classes. For examples, bounds have been known for independent identically distributed (i.i.d) scalar sources with Gaussian, Laplacian, or generalized Gaussian distributions. However, those bounds are derived from the high rate and large block size approximations and may not be tight for situations of practical usage (e.g., low rate and small block size). Moreover, to derive bounds, one needs to first characterize the sources and this can be problematic for complex sources that can be considered as a class of sources characterized by their statistical properties.

To solve the problem of complex source representation such as video, a specific coding framework that can efficiently capture the relevant statistical dependencies and accommodate different types of sources is prerequisite. International video coding standard such as H.264/AVC is proposed to supply the need of specific coding framework. For a given standard-compliant coding framework, we can define an operational R-D curve obtained by applying all possible quantization choices on this input video source. Note that these points are operational in that they are directly chosen, and thus the optimal performance is achievable. In contrast, the bound given by Shannon's theoretical R-D function gives no constructive procedure for attaining the optimal performance.

Fig. 2.2 presents the individual admissible operating points. The boundary between achievable and non-achievable regions is defined by the convex hull of the set of operation points. Hereafter, we will consider optimality in the operational sense.

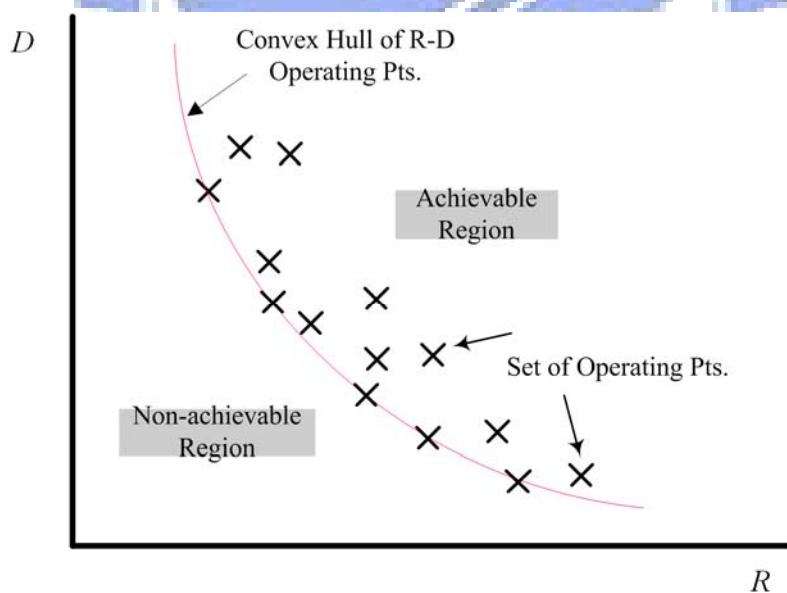


Fig.2.2. An illustration of Operational R-D Characteristic.

In the spirit of operational R-D, we define the “optimal” solution as that achieving the best R-D performance among all possible operating points. More specifically, we find the optimal quantizer, or operating point, for each coding unit such that the goal of minimizing the overall distortion constrained by a given total bit budget is achieved.

## 2.3 Rate-Distortion Optimization Criteria

To achieve the optimal R-D performance on a specific coding standard, the so-called *rate control* algorithms are proposed to determine the best quantization parameter (QP) for a coding unit (which can be a macroblock (MB) or a frame) and these algorithms should also prevent the buffer(s) from underflow or overflow in the environment of a constant bit rate (CBR) channel or a variable bit rate (VBR) channel [34]. There are two commonly used optimization criteria in designing a rate control algorithm for a given bit rate: minimum the average or total distortion (the MINAVE criterion) and minimum the maximum source distortion (the MINMAX criterion).

The MINAVE minimizes the average distortion at the cost of large temporal quality variation, especially for videos with high motion and frequent scene changes. To achieve a visually pleasing video presentation, not only does each video frame need to be encoded at the highest quality level, but also the frame-by-frame perceptual quality change need to be smooth. In fact, the MINMAX criterion is a good choice, when the goal is to achieve an almost constant distortion. However, the MINMAX seldom pays attention to minimize the total distortion.

Also the MINAVE achieves the minimum total distortion at the expense of a larger localized distortion, especially in the areas of long boundary and small objects. As shown in Fig. 2-3, three pictures are presented to illustrate the difference between MINAVE and MINMAX. Simulation results show that the MINAVE approach has a larger localized distortion in red circle. With the MINMAX approach, this problem does not exist since the local maximum allowable distortion is explicitly bounded.

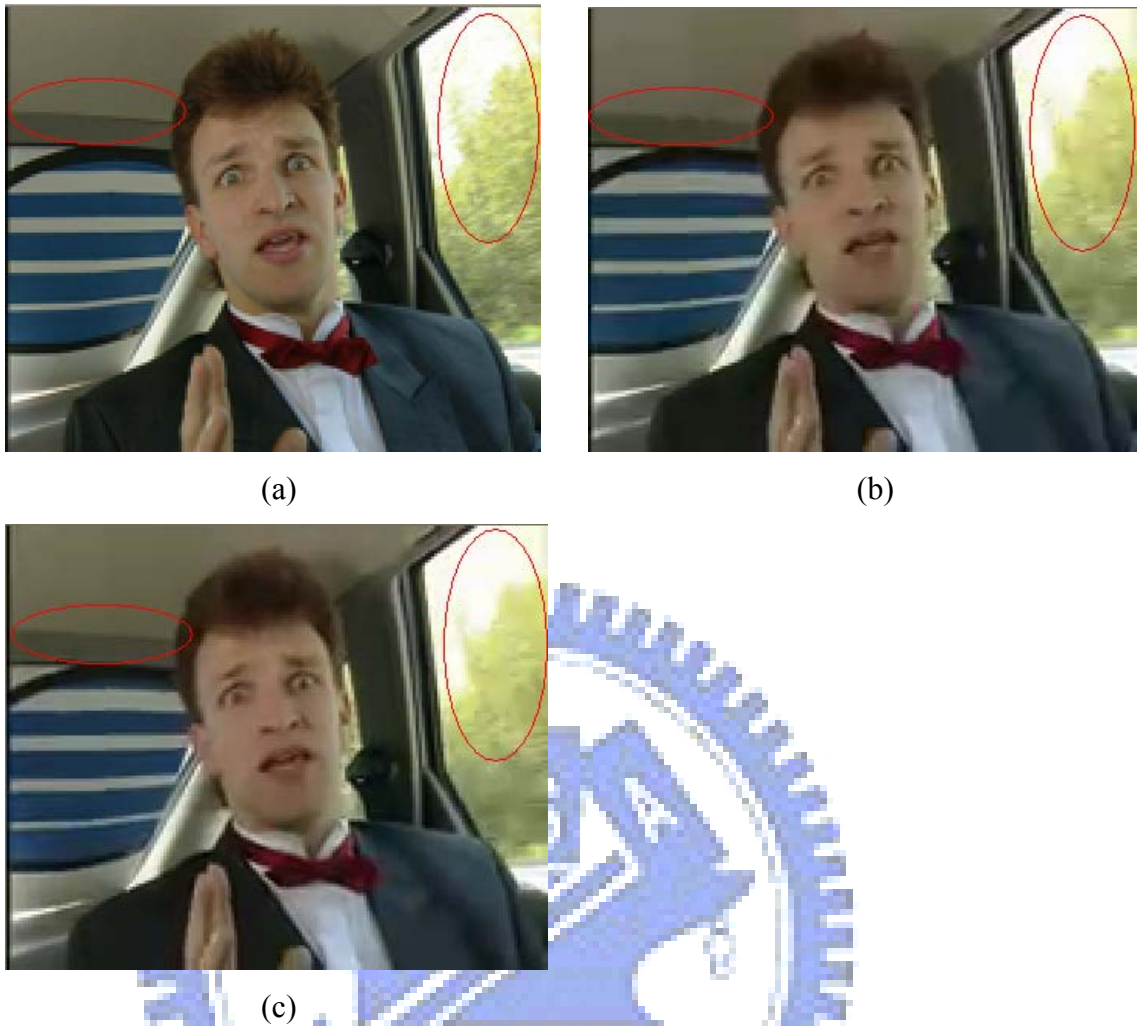


Fig.2.3. Comparison of frame 248 coding results on the Carphone sequence between MINMAX and MINAVE results. (a) original. (b) MINAVE result. (c) MINMAX result.

## 2.4 Trellis Representation of the Tree Structure

In the dependent coding structure, the current frame distortion and bits depend not only on the current QP but also on the previous frame QPs. Given 52 possible QP values, there are 52 possible coded pictures (each coded using a different QP value) for the first frame. Each coded picture is associated with a (distortion, rate) pair after coding. Each of them leads to 52 possible second-frame pictures. Therefore, there are in total  $52^2$  possible pictures (or states, nodes in a tree) for the second picture. The picture (or state) number grows exponentially as more frames are coded. All the possible picture sequences thus form a tree structure.

Two approaches were suggested to reduce the growing number of states. The state pruning technique was proposed by [9] and the state clustering approach was proposed by [11]. In the first approach [9], the state in a tree is denoted by the accumulated frame coded bits. The theoretical basis of state pruning is the “monotonicity” assumption that a better current coding frame will lead to a more efficient coding in the future. Although this monotonicity condition is not always guaranteed as pointed out by [35], our experimental results indicate this assumption is typically true. Therefore, the Markovian condition (the future optimal path depends only on the current state not the previous one) is created. The Viterbi Algorithm (VA) can thus be applied. As a result, when multiple branches arrive at the same state, only one branch of the least cost is selected as the survivor and the complexity is largely reduced. The second complexity reduction approach adopts the notion of “cluster” [11], which merges a few neighboring nodes (states) into one cluster (a state) because these nodes in one cluster have similar characteristics and thus lead to similar final results. Because there are only a finite number of states, the tree structure is degenerated into the trellis structure.

## 2.5 Rate-Distortion Optimization Techniques

In this section, we briefly introduce Lagrange multiplier, Lagrange relaxation, and dynamic programming techniques which are usually employed to optimize the R-D performance.

### 2.5.1 Lagrange Multiplier

Generally the Lagrange multiplier method is employed to transform the constrained problem into an unconstrained problem. Let  $Q$  be the set of quantization parameter values. Given  $K$  frames and a total bit budget  $R_T$ , the constrained problem is to minimize the overall distortion  $D$  by choosing the optimal frame-level QP values  $\mathbf{q}^* = \{ q_0^*, q_1^*, q_2^*, \dots, q_{K-1}^* \}$  for all  $K$  frames,

where  $q_k^* \in Q$ , for  $k=0,1,\dots,K-1$ . Therefore, the constrained problem can be expressed as follows:

$$\min_{q_k \in Q} D = \sum_{k=0}^{K-1} d_k(q_0, q_1, \dots, q_k), \quad \text{s.t.} \quad R = \sum_{k=0}^{K-1} r_k(q_0, q_1, \dots, q_k) \leq R_T, \quad (2.1)$$

where  $d_k$  and  $r_k$  are the  $k$ th frame distortion and bits.

The Lagrange multiplier method introduces a Lagrange multiplier  $\lambda$ , a non-negative real number, to form the Lagrangian cost  $J(\lambda) = \sum_k (d_k + \lambda r_k)$ . We thus formulate the Lagrangian cost minimization as follows:

$$\text{Min}_{q \in Q^K} J(\lambda) = \text{Min}_{q_k \in Q} \sum_{k=0}^{K-1} (d_k + \lambda r_k). \quad (2.2)$$

It is well-known that the optimal solution to the minimizing distortion problem with budget constraint in (1), is equivalent to minimizing Lagrange cost problem,  $\text{Min} J(\lambda^*)$  in (2) with  $R(\lambda^*) = R_T$ . With independent coding assumption, the unconstrained problem can be efficiently solved and formulated as follows:

$$\text{Min}_{q \in Q^K} J(\lambda) = \text{Min}_{q_k \in Q} \sum_{k=0}^{K-1} (d_k + \lambda r_k) = \sum_{k=0}^{K-1} \text{Min}_{q_k \in Q} (d_k + \lambda r_k). \quad (2.3)$$

The key step in finding the optimal solution is to identify  $\lambda^*$ . Sweeping  $\lambda$  from 0 to  $\infty$  will generate the entire convex hull of achievable distortion rate pairs. In general, this optimal  $\lambda^*$  solution can be iteratively solved. The main problem with the Lagrange multiplier method is that the only solutions which belong to the convex hull can be found.

## 2.5.2 Lagrange Relaxation

Lagrange relaxation is a generalization of the use of Lagrange multiplier in classical optimization problems. Given a constrained optimization problem  $X$  with multiple constrains (complicating constrain), this problem may be NP-hard. With Lagrange Relaxation concept,

we say that the constrained problem Y is a relaxation of problem X if Y is obtained from X by eliminating one or more constraints.

The optimal solution obtained from Lagrange relaxation method may be a suboptimal solution to the original problem with complicating constraints. On the other hand, if the solution satisfies the complicating constraint, it is optimal for the original problem. In this thesis, we partition the complicating constraint into different subsets of simple constraints and then iteratively solve the problem with one subset. Thus the solution obtained from the Lagrange relaxation concept is still an optimal one.

### **2.5.3 Dynamic Programming**

As noted previously, the Lagrange multiplier method has the drawback of not being able to reach the optimal point that does not reside on the convex hull of R-D curve. One method that can reach the optimal point that does not reside on the convex hull of R-D curve is the dynamic programming technique.

In general, trellis-based dependencies arise in cases where the memory in the underlying system is finite, i.e., the number of states is finite. In a trellis-based structure, each stage corresponds to a coding unit and each node often represents the cumulative coded bits. One branch expansion is performed by encoding the current coding unit with a particular quantizer and often accompanied with a branch cost. When multiple branches arrive at the same node, only one branch of the minimal cost is selected as the survivor.

The dynamic programming is a technique to find the minimum cost path in a trellis. Since the dependency in the video coding forms a tree structure and each node is defined as a state in this thesis, a trellis representation of the tree structure is executed in order to use this technique. By traversing the trellis from the root to the leaves, we can get successive bit allocation for each coding unit and finally obtain the best picture sequence.



## 2.6 Joint Source-Channel Coding

The problem of transmitting video signal involves both source coding and channel coding. Date back to Shannon's separation principle, one can theoretically separate the source and channel coding tasks with no performance loss. This principle is derived from the large block size and computational resource assumptions. It is obvious that such conditions are not met in practice. Moreover, the available channel capacity is highly time-varying such as the network congestion in network applications and fading in wireless communication applications. Therefore, the closer interaction between source and channel coding functions may be needed to obtain more performance gain. More specifically, the total bit budget come from the channel capacity shall be appropriately allocated between source coding and channel coding. Furthermore, the capability to accommodate the time-varying channel with graceful performance variation is prerequisite for both source and channel coding tasks.

Because coded bit streams to be transmitted have different error protection needs and the available channel capacity is time-varying, the channel coding must accommodate the time-varying bit budget and behave with graceful performance variation. For example, the rate-compatible punctured convolutional (RCPC) code is promising for many application [37]. Serially concatenated with the Reed-Solomon (RS) code, the performance of forward error correction (FEC) system is investigated for both additive white Gaussian noise (AWGN) channel and the fully interleaved Rayleigh fading channel (FI-RFC) [38]. Further details are shown in Appendix A.

Similarly given the continuously time-varying budget bits, the source coding has to encode the video sequence at the highest quality and the frame-by-frame quality change needs to be smooth for video transmission applications. We focus on the "graceful degradation" study in Chapter 4. Simulation results show that the goal of graceful quality variation can be achieved.

# Chapter 3

## Consistent Quality Control Algorithms

In this chapter, we describe the proposed consistent quality control algorithms [36]. In Section 3.1, we introduce the rate-control problem in video coding and derive an equivalent condition between the distortion minimization problem and the budget minimization problem. Two proposed algorithms are described in Section 3.2: a) the trellis-based algorithm with Viterbi search and b) a Lagrangian-based iterative algorithm with bisection search. Section 3.3 presents the simulation results to show the effectiveness of our algorithm. These results are compared with existing MINAVE and MINMAX schemes. Also, the effect of control parameters on PSNR and complexity is studied. Section 3.4 summarizes the findings and their limitations.

### 3.1 Problem Formulation and Distortion-Rate

#### Function

The frame-level bit allocation problem and the uniqueness property of the distortion-rate function are described in this section. In our selected structure, we encode a frame and all its macroblocks using the same QP. The notion of quality in this thesis is the well adopted image objective criterion, PSNR.

#### 3.1.1 Dependent MINAVE Bit Allocation Problem

In the (forward prediction) dependent coding formulation, the  $k$ th frame distortion and bits, i.e.,  $d_k$  and  $r_k$ , depend on the current and previous frame QP values. Let  $Q = \{0, 1, \dots, 51\}$  be the set of quantization parameter values in the H.264 standard video codec. Given  $K$  frames and a

total bit budget  $R_T$ , our goal is to minimize the overall distortion  $D$  by choosing the optimal frame-level QP values  $\mathbf{q}^* = \{q_0^*, q_1^*, q_2^*, \dots, q_{K-1}^*\}$  for all  $K$  frames in a sequence, where  $q_k^* \in Q$ , for  $k=0,1,\dots,K-1$ . That is,

$$\mathbf{q}^* = \arg \min_{q_k \in Q} D = \sum_{k=0}^{K-1} d_k(q_0, \dots, q_k), \quad (3.1)$$

subject to the constraints

$$R = \sum_{k=0}^{K-1} r_k(q_0, \dots, q_k) \leq R_T, \text{ and}$$

$$|f(d_k) - f(\bar{D})| \leq \delta_p, \forall k \in \{0, 1, \dots, K-1\},$$

where  $\bar{D}$  is the average distortion for all  $K$  frames and  $f(\cdot)$  is the PSNR function calculated by  $f(d) = 10 \log_{10}(255^2 \times FPN/d)$ , where  $FPN$  is the pixel number in a frame. The second constraint in (3.1) is added to achieve the consistent quality video; that is, the difference between the frame PSNR and the average sequence PSNR is limited by  $\pm\delta_p$ .

Another important function of a rate control algorithm is to avoid the buffer underflow and overflow problems. The MPEG standard imposes a hypothetical decoder model on a legal bit stream, namely, Video Buffer Verifier (VBV). There are three prescribed operation modes in VBV. In this study, we consider only the constant bit rate (CBR) mode; i.e., the channel rate is constant. We assume that the decoder buffer is large enough to eliminate the buffer overflow problem. In more details, the buffer is initially empty. To avoid the buffer underflow problem, bits in the decoder buffer accumulate for a specific time before the bits of the first frame are removed. Afterwards, the decoder buffer continues receiving constant-rate bits from the channel and the decoder removes the bits in buffer at regular frame-time intervals. Essentially, the buffer underflow problem imposes a delay  $T_d$  on the decoder. For frame  $k$ , the buffer occupancy is

$$B_k = B_0 + kc - \sum_{i=0}^k r_i = T_d c + kc - \sum_{i=0}^k r_i, \quad (3.2)$$

where  $B_0$  is the initial buffer occupancy and  $c =$  channel bit rate/frame rate. The buffer underflow is avoided if the constraint  $B_k \geq 0$  for all  $k \geq 0$  is satisfied. In other words, the decoder delay  $T_d$  shall be selected to ensure that the buffer contains at least  $r_k$  bits, when the decoder starts decoding frame  $k$  for all  $k \geq 0$ .

### 3.1.2 Uniqueness of Distortion-Rate Function

In the conventional MINAVE problem, we minimize the total distortion subject to a given bit constraint. However, in order to achieve a consistent quality video, it is more convenient if the distortion, not the bit rate, is the controllable argument in our process. That is, we prefer  $MinR(D_T)$  rather than  $MinD(R_T)$ .

In the classical information theory, the distortion-rate function,  $D(R)$ , is a nonincreasing, convex function and its slope must be both nonpositive and nondecreasing. Then, the rate-distortion function,  $R(D)$ , the inverse of  $D(R)$ , is a legal nonincreasing, convex function too. As a result, the solution to the  $MinR(D_T)$  problem is identical to that to the  $MinD(R_T)$  problem. However, these ideal properties of the rate-distortion function may not true for the real-data case. Therefore, we study the relation of these two solutions in the operational sense and derive the proposition as follows.

**Proposition:** Given a rate-distortion coder with control parameters of discrete and finite values, we consider the operational  $R(D)$  and  $D(R)$  functions. In other words,  $D(R)$  is the achievable distortion for the given bit rate  $R$ .  $R(D)$  is similarly defined. Then, *the optimal solution,  $(D_0^*, R_0)$ , to the minimum distortion problem, i.e.,  $MinD(R_T)$ , is also the optimal solution,  $(D_1, R_1^*)$ , to the minimum budget problem, i.e.,  $Min R(D_T=D_0^*)$ , if the optimal distortion function  $D^*(R)$  is a one-to-one mapping, where  $(D^*, R)$  is the solution set to the Min*

$D(R_T)$  problem at the given  $R_T$  budget bits.

**Proof :**

Since  $(D_I, R_I^*)$  is the optimal solution to  $\text{Min}R(D_T=D_0^*)$ , it implies  $D_I \leq D_0^*$ . On the other hand,  $D_0^*$  is the optimal solution (least amount of distortion) to  $\text{Min}D(R_T)$ , thus  $D_I \geq D_0^*$ . Consequently, we have  $D_I = D_0^* = D_T$ . The optimal solution  $(D_0^*, R_0)$  of  $\text{Min}D(R_T)$  implies  $R_0 \leq R_T$ . In addition,  $R_I^*$  is the optimal solution (least amount of bits) of  $\text{Min}R(D_T=D_0^*)$ ; it thus implies  $R_I^* \leq R_0$ . Consequently, we have  $R_I^* \leq R_0 \leq R_T$ . Now, if  $D^*(R)$  is a one-to-one function, the relation  $R_I^* = R_0$  must be true because  $D_I = D_0^*$ . Therefore, the solutions to these two problems,  $\text{Min}R(D_T=D_0^*)$  and  $\text{Min}D(R_T)$ , are identical if  $D^*(R)$  is a one-to-one function. (QED).

## 3.2 Consistent Quality Control Algorithm

Two approaches are chosen to solve the inter-frame dependent coding problem in this study. We start with the trellis-based approach. First, the tree structure inherent in dependent coding is reduced to the trellis structure. Then, the branch expansion process is described and the Viterbi search is used to solve the bit allocation problem. Next, a fast branch expansion algorithm extended from a previous proposal is presented. In the last sub-section, we propose the Lagrange multipliers approach. An iterative structure is designed for finding the optimal lambda value in the Lagrange cost. To speed up this iterative process, a couple of the existing but independently proposed fast schemes are included with proper modifications.

### 3.2.1 Trellis-Based Coding Scheme

We adopt both the concepts of monotonicity and cluster in this study. However, for the quality variation control purpose in this study, the distortion value (represented by PSNR) is used as the state variable. In addition, because the PSNR value is a real number, the problem of

infinite states occurs in this formulation. Therefore, a cluster representing a distinct range of PSNR values is defined as a *state*. The *cluster size* parameter  $P_\Delta$  is used to define the span of a cluster. To convert the tree structure into a trellis, it is necessary to restrict the dynamic range of admissible PSNR. It is set by the lowest quality, denoted by  $P_L$ , and the highest quality, denoted by  $P_U$ . This range should include all the PSNR values in the optimal solution and is chosen empirically. Consequently, the number of states equals to  $1 + \lfloor (P_U - P_L) / P_\Delta \rfloor$ , where  $\lfloor x \rfloor$  denotes the integer part of  $x$ . Because there are only a finite number of states, the tree structure is degenerated into the trellis structure. In contrast, the concept of cluster is proposed to reduce the tree search complexity in [11] and now is extended for the purposes of both defining finite states and reducing complexity in this study.

The rest is the detailed description of our trellis structure. Fig. 1 illustrates the relation among cluster, node, branch,  $P_\Delta$ , and  $\delta_P$ .

- **Cluster:** The notation  $c_k^i(R_k)$  represents a cluster with index  $i$  at stage (frame)  $k$ , where  $i \in [0, \lfloor (P_U - P_L) / P_\Delta \rfloor]$  and  $k \in [0, K-1]$ . The  $i$ th cluster PSNR range is  $[P_L + iP_\Delta, P_L + (i+1)P_\Delta)$ . A cluster may contain a number of nodes in it. The best performing node (in the R-D sense) inside a cluster is chosen to be the *representative node* of this cluster.
- **Node:** A node  $n_k^i(D_k, R_k)$  represents a legal operating point of the coding result, whose PSNR value is in the cluster  $i$  at frame  $k$ , where  $i = \lfloor (f(\overline{D}_k) - P_L) / P_\Delta \rfloor$ , and  $\overline{D}_k = D_k / k$ .  $D_k$  and  $R_k$  are the accumulated coded distortion and bits before encoding frame  $k$  respectively.
- **Branch:** A branch connects two nodes in the trellis diagram. The notation  $b_k^{i,j}(q_k)$  indicates that it stems from the representative node in cluster  $i$  at frame  $k$  and it ends at a node in cluster  $j$  at frame  $k+1$ . It uses  $q_k$  to quantize frame  $k$ . It produces a

next stage node  $n_{k+1}^j (D_{k+1} = D_k + d_k^i(q_k), R_{k+1} = R_k + r_k^i(q_k))$ , where  $j = \lfloor (f(\bar{D}_{k+1}) - P_L) / P_\Delta \rfloor$  and  $\bar{D}_{k+1} = D_{k+1} / (k+1)$ , if the three conditions,  $R_{k+1} \leq R_T$ ,  $|f(d_k) - f(\bar{D}_k)| \leq \delta_p$  and  $P_L \leq f(\bar{D}_{k+1}) \leq P_U$  are all satisfied. A rate-distortion pair  $(r_k^i(q_k), d_k^i(q_k))$  is associated with this branch. Note that the average sequence PSNR value  $f(\bar{D})$  is not available until the end of the encoding process. It is thus approximated by the current  $f(\bar{D}_k)$  value.

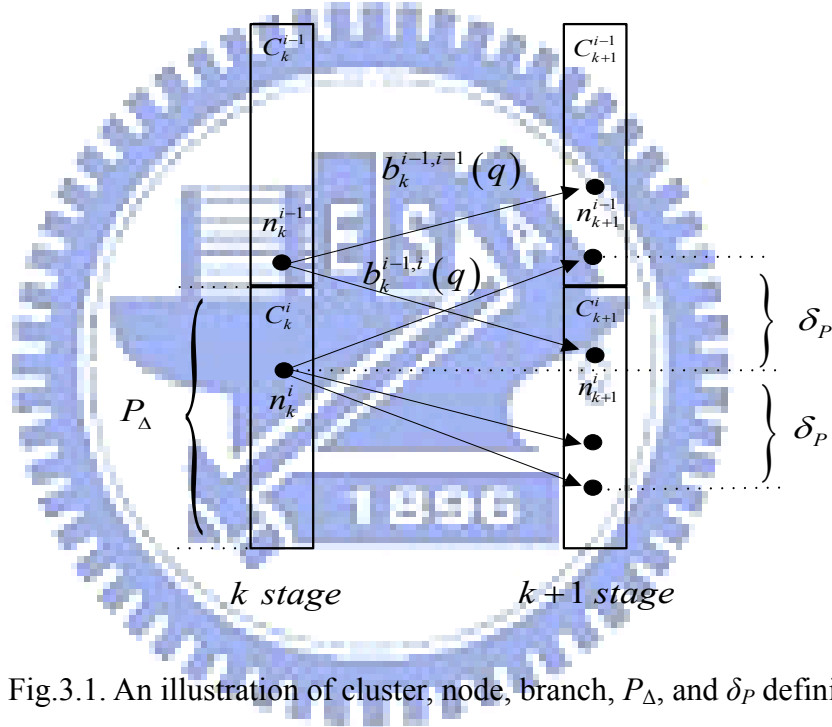


Fig.3.1. An illustration of cluster, node, branch,  $P_\Delta$ , and  $\delta_P$  definitions.

### 3.2.2 Branch Expansion and Frame-level Bit Allocation

Let two nodes of  $n_{k-1}^j$  and  $n_k^i$  be connected by a branch  $b_{k-1}^{i,j}(q_{k-1})$ . In the branch expansion process for node  $n_k^i$ , all the QPs satisfying the following three constraints are examined (that is, they are used to quantize data in frame  $k$ ): a) PSNR range  $P_L \leq f(\bar{D}_{k+1}) \leq P_U$ , b) bit budget  $R_{k+1} \leq R_T$ , and c) quality variation  $|f(d_k) - f(\bar{D}_k)| \leq \delta_p$ . The previous frame QP value,  $q_{k-1}$ , is selected to be the center QP value, denoted by  $QP_c$ , and the examined QPs are

expanded from the center value gradually by  $q_{k,n} = q_{k-1} \pm n$ , where the step index  $n$  is incremented by one until any of the above constraints is violated.

The first frame (I frame) in a sequence is by default the first active node. In the following frames (P frames), the number of branches and nodes grows exponentially if they are not eliminated or merged. The adaptation of the cluster concept allows the merge of nodes with similar distortions. A cluster containing at least one expanding node in it is called *active cluster*. When a small cluster size, say,  $P_{\Delta} \approx 0.1dB$ , is in use, typically only the branch of least accumulated bits and its associated node will be the single survivor in this cluster. The survivor node in an active cluster is defined as an *active node*. The “monotonicity assumption” enables the elimination of weaker branches (branches with higher bit rates) ending at the same node (cluster). That is, in the backtracking process, only the active node with the smallest total distortion and permissible bit usage is selected. Therefore, the goal of minimizing the total distortion is achieved.

To accomplish the consistent quality video goal,  $\delta_P \leq 0.4dB$  is usually adopted. Overall, the proposed quality control algorithm is summarized below.

---

*Algorithm 1: Trellis-based Consistent Quality Control (TCQC) Algorithm*

---

Step 1: Initialize the values of  $R_T, \delta_P, P_L, P_U$ , and  $P_{\Delta}$ .

Step 2: Encode the first I frame using all quantization values. Prune the branches that violate any of the two constraints: the PSNR range  $P_L \leq f(\bar{D}_k) \leq P_U$  and the bit budget  $R_k \leq R_T$ .

Step 3: If multiple branches merge at the same destination cluster, select the branch with the least accumulated bits and its corresponding node becomes the survivor. At the end of this step, each cluster contains only one active node, which is connected to only one surviving branch. Save the context information of the survivor nodes.



Step 4: Expand all active nodes for the next I- or P-frame. Encode the next frame (frame  $k$ ) using all allowable quantization scales. Prune the branches which violate any of the three constraints: the PSNR range  $P_L \leq f(\bar{D}_{k+1}) \leq P_U$ ,  $R_{k+1} \leq R_T$ , and the quality variation constraint  $|f(d_k) - f(\bar{D}_k)| \leq \delta_p$ .

Step 5: If the current frame is not the last frame in the sequence, go to Step 3.

Otherwise, among all active clusters, choose the survivor node with the best overall quality as the final solution. Backtrack along the optimal path connecting to the starting frame of this sequence. We thus obtain the optimal frame-level QP and bits for each frame. This sequence is then done.

### 3.2.3 Fast Branch Expansion Process

Generally, a complete video encoding process is executed whenever a branch is expanded. In the MPEG JM reference software, the coding parameter selection is done by two components: the rate-control algorithm and the rate distortion optimization (RDO) process. This 2-stage coder control structure is well recognized for its efficiency for a highly complicated hybrid video coder such as H.264. But the RDO process is costly in computation. The RDO process needs a QP input value for its operation and it outputs the coding modes, distortion, header bits, and residual signals. On the other hand, a typical rate-control algorithm needs the modes etc. information to pick up the best QP for quantizing the current MB or frame. Therefore, these two components depend on each other for supplying their inputs, a chicken and egg problem [22]. Let  $QP_1$  and  $QP_2$  denote the QPs used by the RDO process and the quantization process, respectively. The initial value of  $QP_1$  is generally not equal to the value of  $QP_2$ . Therefore, an iterative procedure has been proposed for updating  $QP_1$  (for example,  $QP_{1\text{new}} = (QP_1 + QP_2)/2$ ) after the first set of  $QP_1$  and  $QP_2$  are obtained [22].

It is reported that the coding PSNR loss is less than 0.2 dB when  $|QP_1 - QP_2| \leq 3$  [22].

When a frame is encoded twice using two sets of QP values, namely,  $QP_1=QP_2= q_1$  and  $QP_1=QP_2= q_2$ , separately, we run RDO only once with  $QP_1 =q_1$ . Using the aforementioned property, the same RDO outputs are used for quantization in both cases,  $QP_2 = q_1$  and  $QP_2 = q_2$ , if  $q_1$  and  $q_2$  are sufficiently close. We thus save one RDO computation.

To lower the approximation error, we restrict the approximation range by  $|QP_1 - QP_2| \leq 2$ . The fast branch expansion process now runs as follows. First, the current frame is encoded using the center QP defined in Section III-B, i.e.,  $QP_1=QP_2=QP_c$ . Then, the upper and lower two branch expansions can be easily generated by performing the quantization processes four times with  $QP_2=QP_c\pm 1$ ,  $QP_2=QP_c\pm 2$ . As a result, five branch expansions are generated at the cost of computing one RDO process and five quantization processes. If more branch expansions are needed, another complete video encoding process is needed, for example,  $QP_1=QP_2=QP_c+5$  or  $QP_c-5$ . Finally, to prevent the approximation error propagation to the next stage, a complete video encoding process, i.e., running RDO and quantization with the chosen final QP, is executed again for each active cluster.

### 3.2.4 Technique based on the Lagrange Multipliers

Another optimization technique, the so-called *Lagrange multipliers method* can also be used to find the optimal operation point on the rate-distortion curve [11]. We define the Lagrange cost to be  $J(\lambda) = \sum_k d_k + \lambda r_k = \sum_k J_k(\lambda)$ . The goal becomes

$$\text{Min}_{q \in Q^K} J(\lambda) = \text{Min}_{q_k \in Q} \sum_{k=0}^{K-1} (d_k + \lambda r_k) = \sum_{k=0}^{K-1} \text{Min}_{q_k \in Q} (d_k + \lambda r_k). \quad (3.3)$$

It is well-known that the optimal solution to the minimizing distortion problem with budget constraint, denoted by  $\text{Min}D(R_T)$ , is equivalent to that of minimizing the Lagrange cost,  $\text{Min} J(\lambda^*)$  in (3.3) with  $R(\lambda^*) = R_T$  [11]. The key step in finding the optimal solution is to identify  $\lambda^*$ , the optimal value of lambda. In general, this optimal  $\lambda^*$  solution can be iteratively

solved [11]. However, in this study, we impose two additional constraints: the consistent quality constraint,  $|f(d) - f(\bar{D})| \leq \delta_p$  and the PSNR range constraint,  $P_L \leq f(\bar{D}) \leq P_U$ . We develop an iterative process to solve this new and more complex problem as follows.

First, the budget constraint of  $R(\lambda^*) = R_T$  is relaxed. We intend to find a proper lambda range, denoted by  $[\lambda_{LL}, \lambda_{UU}]$ , such that the solution to the  $\text{Min } J(\lambda)$  problem with a lambda located inside this range shall satisfy all three constraints,  $P_L \leq f(\bar{D}) \leq P_U$ ,  $|f(d) - f(\bar{D})| \leq \delta_p$ , and  $R(\lambda_{UU}) < R_T < R(\lambda_{LL})$ . Therefore, the optimal lambda value  $\lambda^*$  is guaranteed to locate in the selected range. Next, a fast bisection algorithm in [30] is employed to find the solution to the  $R(\lambda^*) = R_T$  problem. That is, the lambda search process iterates until the predefined bit rate tolerance, i.e.,  $R_T - R(\lambda)/R_T \leq \varepsilon$ , is satisfied. And the (optimal) QPs are a byproduct in this process.

In the following, we describe how the constraints are satisfied in the aforementioned process of finding the lambda range. For a given frame, we examine only the valid QP values that satisfy the quality constraint,  $|f(d) - f(\bar{D})| \leq \delta_p$ . The picture coding process is similar to the fast branch expanding step described earlier. To satisfy the other two constraints  $P_L \leq f(\bar{D}) \leq P_U$  and  $R(\lambda_{UU}) < R_T < R(\lambda_{LL})$ , we start with two initial lambda values,  $\lambda_U$  and  $\lambda_L$ , such that both  $R(\lambda_U) < R_T < R(\lambda_L)$  and  $[P_L, P_U] \subset [P(\lambda_U), P(\lambda_L)]$  are satisfied. Then, the center value in the current lambda interval is used as the *test lambda*  $\lambda_T$  to determine whether the solution to the  $\text{Min } J(\lambda_T)$  problem satisfies the constraint  $P_L \leq f(\bar{D}(\lambda_T)) \leq P_U$ . If the current average PSNR is lower than  $P_L$ , a smaller lambda should be used and thus the lower subinterval  $[\lambda_L, \lambda_T]$  is selected as the lambda interval for the next iteration. Equivalently, the test lambda value is decreased in the next iteration. On the other hand, if the current average PSNR is larger than  $P_U$ , the upper subinterval  $[\lambda_T, \lambda_L]$  is selected as the lambda interval for the

next iteration, which increases the test lambda value in the next iteration. We check the average PSNR value whenever a frame is coded. If either of the above conditions happens, we need to re-encode the video sequence from the first frame again using the new lambda range. This process continues until the chosen  $\lambda_T$  leads to a successful coding of the entire video sequence. At the end, if the resulting bits are smaller than the bit budget, the latest test lambda value is referred as  $\lambda_{UU}$ . The same process is performed in the lambda interval  $[\lambda_T, \lambda_{UU}]$  to obtain  $\lambda_{LL}$  value, but note that the obtained  $\lambda_{LL}$  value shall satisfy  $R(\lambda_{LL}) > R_T$ . Theoretically, if the values of  $P_L$ ,  $P_U$ ,  $\lambda_L$ , and  $\lambda_U$  are properly selected (so that the optimal solution exists), because the R-D curve is convex, this algorithm converges. Overall, the iterative lambda optimization steps are summarized below.

---

*Algorithm 2: Lagrange-based Consistent Quality Control (LCQC) Algorithm*

---

- Step0: Start with two values  $\lambda_U$  and  $\lambda_L$  such that  $R(\lambda_U) < R_T < R(\lambda_L)$  and  $[P_L, P_U] \subset [P(\lambda_U), P(\lambda_L)]$ . Set  $\lambda_T = (\lambda_L + \lambda_U)/2$  and frame index  $k=0$ .
- Step1: Given  $\lambda_T$ , use the fast branch expansion technique to examine all the QPs that satisfy  $|f(d_k) - f(\bar{D}_k)| \leq \delta_p$ .
- Step2: If  $P_L \leq f(\bar{D}(\lambda_T)) \leq P_U$ , go to Step 3. Else if  $f(\bar{D}(\lambda_T)) > P_U$ , set  $\lambda_L = \lambda_T$ ; otherwise ( $f(\bar{D}(\lambda_T)) < P_L$ ), set  $\lambda_U = \lambda_T$ . Let  $\lambda_T = (\lambda_L + \lambda_U)/2$ ,  $k = 0$  (start from the first frame again), go to Step 1.
- Step3: Encode the current frame again using the up-to-date QP value. If the current frame is not the last frame in the sequence, let  $k = k+1$ , go to Step 1.

Step4: If  $R(\lambda_r) < R_r$  set  $\lambda_{uu} = \lambda_u = \lambda_r$ . Else set  $\lambda_{ll} = \lambda_l = \lambda_r$ . If the lambda interval boundaries,  $\lambda_{ll}$  and  $\lambda_{uu}$ , are both found, go to Step 5. Else let  $\lambda_r = (\lambda_l + \lambda_u)/2$ ,  $k = 0$ , go to Step 1.

Step5: Perform the fast bisection search algorithm [30] in the lambda range  $[\lambda_{ll}, \lambda_{uu}]$  to find the optimal  $\lambda^*$ , i.e.,  $R(\lambda^*) = R_r$ . The usual stop rule  $R_r - R(\lambda)/R_r \leq \varepsilon$  is adopted. A few assistant formulas are proposed in [30] so that this search process converges rather fast. Normally, this step takes 2 to 4 recursions. The final  $\lambda^*$  and its associated QPs are our optimal solution.

Typically, Steps 1 and 3 require only one branch expansion process (to examine the valid QPs) and one complete encoding process (to prevent approximation error propagation), respectively. The computational complexity mainly comes from the number of iterations. It usually takes 5 to 8 iterations to complete this lambda search. Detailed simulation results including PSNR and computing time are discussed in Section 3.3.

### 3.3 Simulation Results

We have implemented the proposed quality control algorithm on MPEG-4 AVC/H.264 video coder with the rate-distortion optimization (RDO) option turned on. Experiments are performed using the standard MPEG video sequences, *Foreman*, *Table Tennis*, *News*, and *Stefan*. All test videos are 300 frames in QCIF size. The GOP size is 30. Only I- and P- frames are in use. The PSNR range in each case is estimated from the minimum PSNR and the maximum PSNR obtained by applying JM 7.6 to the test video sequence. Simulations are performed on a 3-GHz Intel Pentium CPU.

We conduct four sets of simulations to evaluate performance of the proposed TCQC and LCQC algorithms. In the first experiment, the TCQC algorithm is tested at different bit rates

to show its effectiveness on bit allocation, as compared with the JM and the constant QP schemes. The JM7.6 rate control scheme is unable to select a QP for the first frame. For fair comparison, the first QP is set to be identical to that of the TCQC algorithm. Also, the best constant QP case is shown, which is produced by using a single QP value for the entire sequence. In this experiment, all possible QP values are tried and the one which produces bits closest to the target bits is chosen. Next, the PSNR and complexity of the LCQC algorithm are compared with two published algorithms, LPF in [24] and MultiStage in [27]. In the third and fourth experiments, TCQC and LCQC are compared. Several  $\delta_P$  and  $P_\Delta$  values are tested to show the PSNR and complexity tradeoff.

### 3.3.1 Performance Comparison with Constant QP and JM

The TCQC algorithm is evaluated on four different video sequences at three different bit rates to show its effectiveness on bit allocation. The *Foreman* sequence contains mainly a talking head with a scene change near the end, the *News* sequence contains some amount of background changes, the *Table Tennis* sequence has a scene change in the middle, and the *Stefan* sequence has high motion. Two other schemes, namely, JM 7.6 and constant QP, are also applied to these sequences. The parameters used in this experiment are the cluster size  $P_\Delta=0.1$  dB and the maximal quality variation  $\delta_P=0.4$  dB. The PSNR curves and their relative merits of these three schemes show similar trend on all these four test sequences and thus only the *Foreman* and *News* sequences are displayed in Tables 3.1 and 3.2. The *News* plot which has the largest variation is also displayed in Fig. 3.2.

As shown in Tables 3.1 and 3.2, the TCQC scheme has the least PSNR variation as compared to JM and constant QP. It has the highest minimum PSNR and the lowest maximum PSNR. The constant QP method is the simplest conceptually but its overall PSNR is often lower; it has pretty low PSNR variation but not the lowest. Generally, the complexity of constant QP method is much lower than that of TCQC. To ensure a consistent frame-by-frame

quality, TCQC has a lower PSNR than JM 7.6, but the difference is often less than 0.5 dB. As shown in Subsection 3.3.3, the average PSNR gets higher if the  $\delta_P$  constraint is loosen. Also shown in Tables 3.1 and 3.2 are the decoder buffer delay ( $T_d$  defined in (2)), which avoids buffer underflow.

Table 3.1. Comparisons of Minimum PSNR, Maximum PSNR, Average PSNR, PSNR Variance, Bit Rate, and Decoding Delay for JM 7.6, TCQC, and Constant QP Schemes on the Foreman Sequence.

Target Rate	Method	Rate(% error)	PSNR(dB)				Delay(s)
			Min	Max	Avg	Var	
24 kbps	JM7.6	24.05 (+0.20%)	22.53	30.37	26.35	3.32	0.43
	TCQC	23.83 (-0.73%)	25.62	27.15	26.11	0.07	0.73
	Fixed QP=46	22.11 (-7.86%)	24.42	28.70	25.81	0.49	0.20
64 kbps	JM 7.6	64.10 (+0.15%)	25.46	35.35	32.30	2.99	0.30
	TCQC	63.38 (-0.97%)	31.76	33.09	32.30	0.04	0.67
	Fixed QP=36	58.50 (-8.59%)	30.24	33.79	31.91	0.77	0.40
112 kbps	JM7.6	112.04 (+0.04%)	30.60	38.46	35.43	2.26	0.33
	TCQC	111.46 (-0.48%)	34.92	36.47	35.38	0.06	0.40
	Fixed QP=31	104.97 (-6.28%)	33.15	36.79	35.09	0.97	0.50

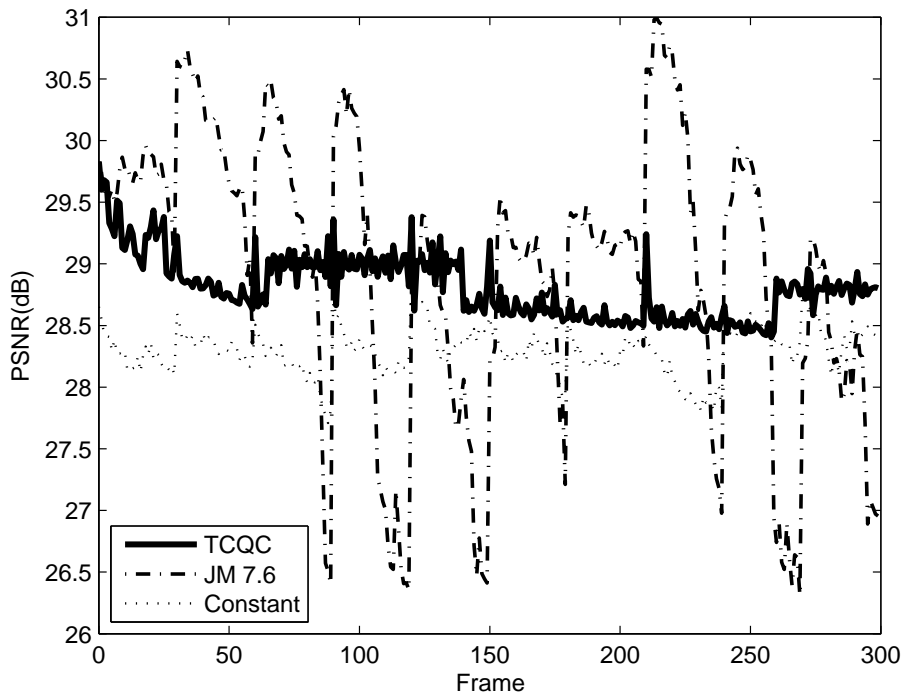
Table 3.2. Comparisons of Minimum PSNR, Maximum PSNR, Average PSNR, PSNR Variance, Bit Rate, and Decoding Delay for JM 7.6, TCQC, and Constant QP Schemes on the News Sequence.

Target Rate	Method	Rate(% error)	PSNR(dB)				Delay(s)
			Min	Max	Avg	Var	
24 kbps	JM7.6	24.19 (+0.79%)	26.31	30.99	28.98	1.36	0.57
	TCQC	23.95 (-0.20%)	28.4	29.83	28.81	0.05	0.43
	Fixed QP=42	22.25 (-7.28%)	27.71	28.91	28.30	0.04	0.33
64 kbps	JM7.6	64.23 (+0.35%)	32.57	38.44	35.46	1.07	0.47
	TCQC	62.95 (-1.65%)	34.39	35.76	34.81	0.04	0.37
	Fixed QP=32	61.62 (-3.72%)	34.39	35.69	34.91	0.06	0.33
112 kbps	JM7.6	112.31 (+0.28%)	36.20	42.20	39.06	0.92	0.37
	TCQC	109.71 (-2.05%)	37.99	39.27	38.41	0.04	0.30
	Fixed QP=27	107.25 (-4.24%)	38.05	39.31	38.45	0.05	0.30

Simulation results also show that our minimum and maximum PSNR values are very

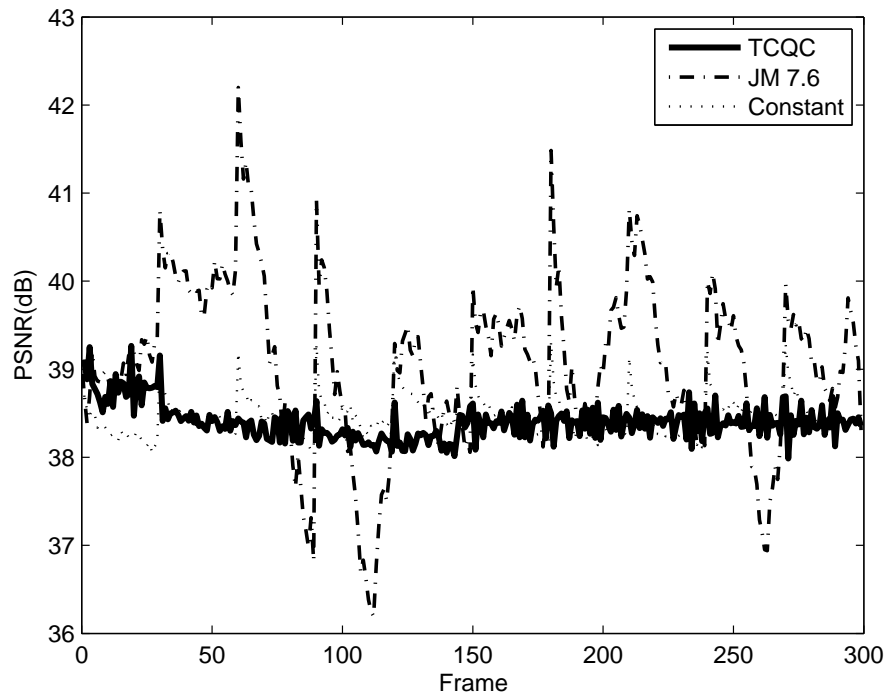
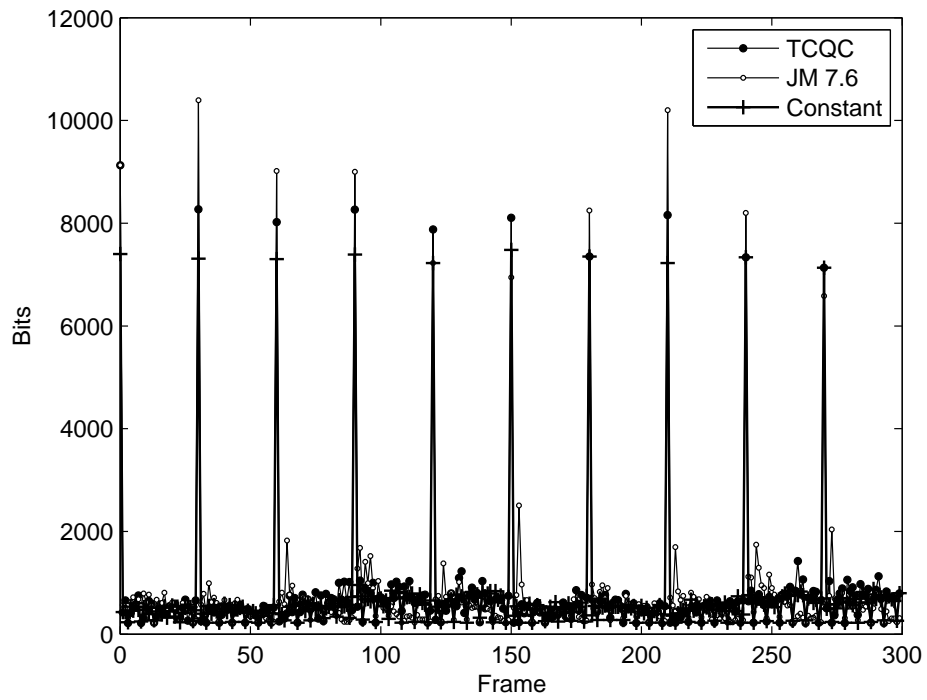
close. Therefore, it is possible to narrow down the PSNR range for further complexity reduction in our algorithm. Empirically the JM average PSNR,  $P_{\text{avg},\text{JM}}$ , is a good estimate for the TCQC average PSNR. Extensive simulation results conclude that typically the PSNR range can be approximated by  $(P_{\text{avg},\text{JM}}-1, P_{\text{avg},\text{JM}}+1)$ .

Fig. 3.2 depicts the frame-by-frame PSNR and used bit plots for the *News* sequence at two different bit rates. The TCQC PSNR curve has no drop at the GOP boundaries or at scene changes. It has the smoothest shape among these three curves. The overall PSNR performance of JM 7.6 is the best but it has a large swing of more than 3 dB in PSNR across the entire sequence. One may notice that the first few frames of the TCQC algorithm have higher PSNR. This agrees with the well-known observation that a good I frame leads to better P frames in a GOP. As discussed earlier, the Viterbi search provides the optimal solution under the given assumptions and constraints. Therefore, although the average PSNR of TCQC is slightly lower than that of JM, TCQC offers the best average PSNR under the consistent quality constraint.

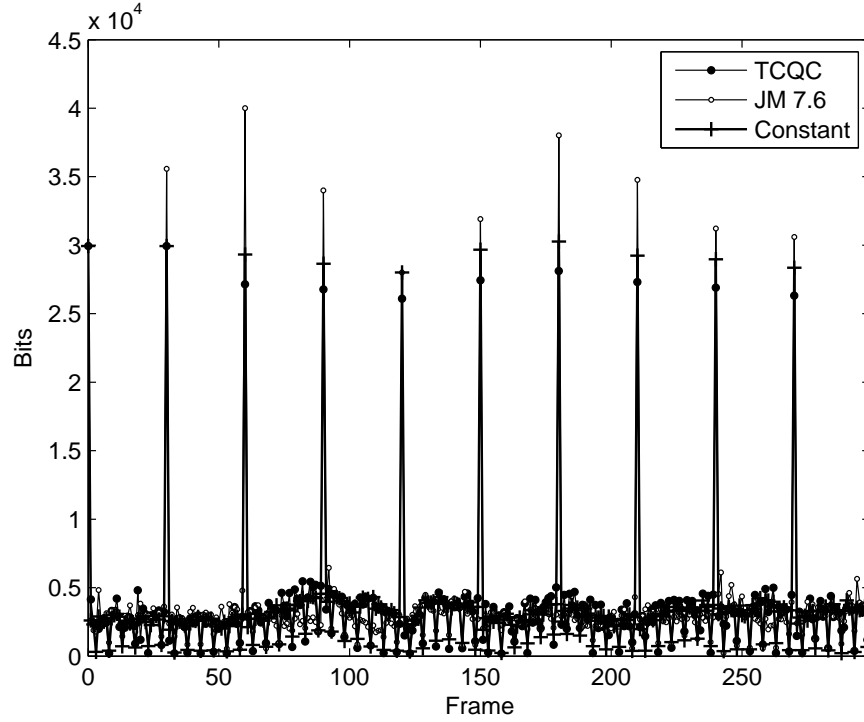


(a)





(c)



(d)

Fig.3.2. PSNR and used bit plots of the TCQC, JM 7.6, and Constant QP algorithms for *News* at two bit rates. (a) PSNR plots at 24 kbps (b) Used bit plots at 24 kbps (c) PSNR plots at 112 kbps (d) Used bit plots at 112 kbps.

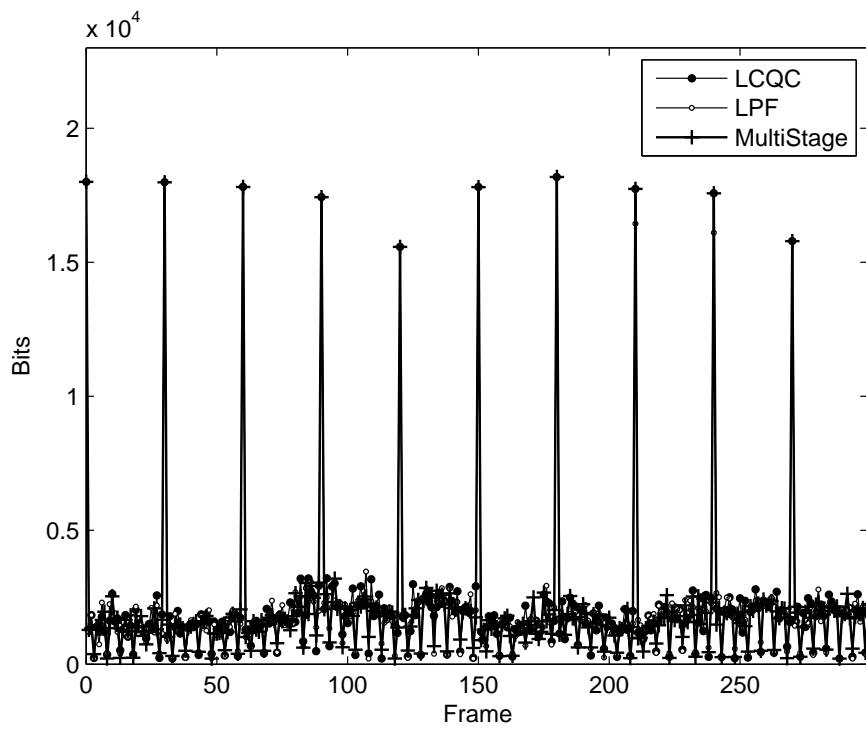
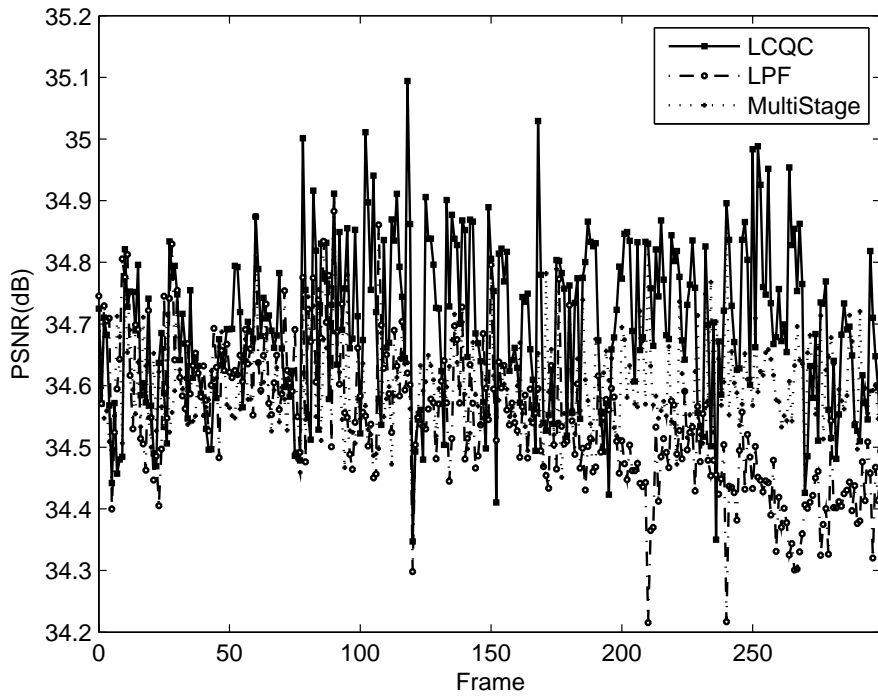
### 3.3.2 LCQC Performance Comparison with LPF and MultiStage Algorithms

In this subsection, two recent well-performed rate-control algorithms, LPF in [24] and MultiStage in [27], are simulated and compared to our LCQC algorithm. The basic idea behind LPF (low-pass filtering) is to smooth out (low-pass filtering) the distortion curve by reallocating the bits of frames inside a moving time window. A quite accurate model that relates the smoothed distortion and the smoothed bit rate is proposed in [24].

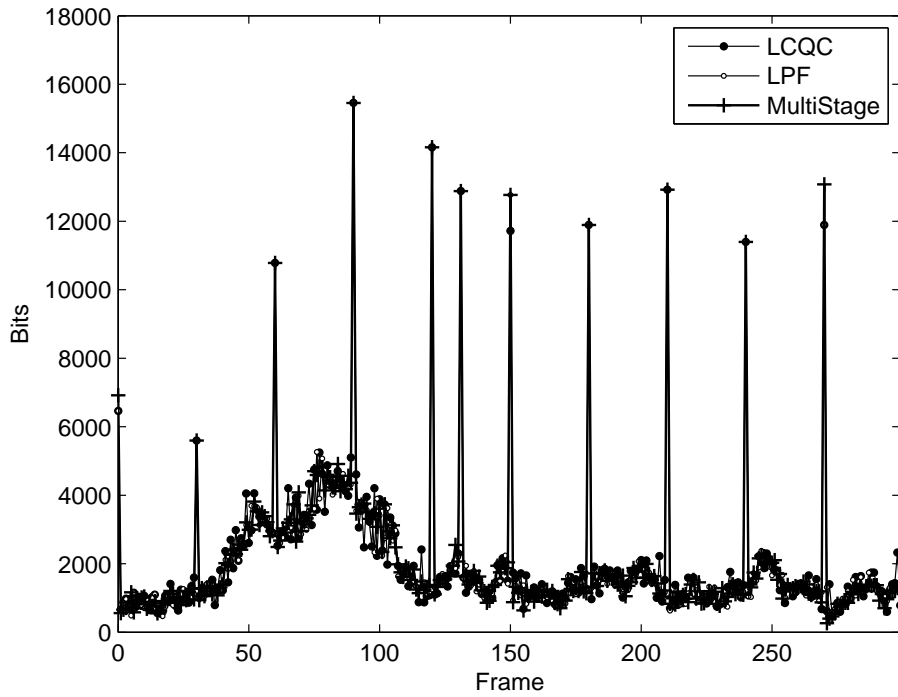
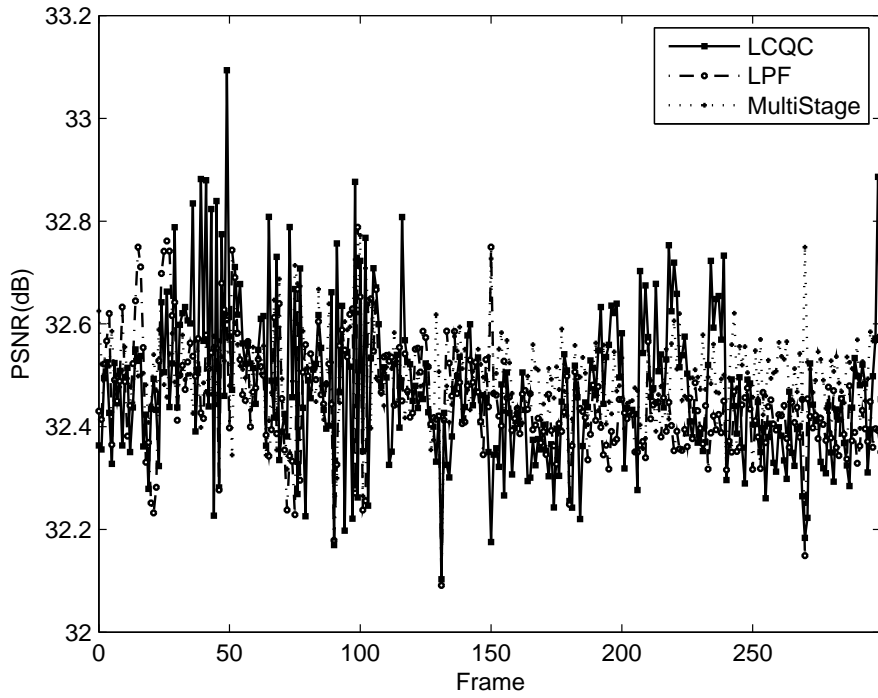
The MultiStage algorithm is aiming at the constant quality target. A 2-stage iterative procedure is proposed [27]. Given a set frame bits, the *Target rate stage* encodes each frame with the given bits. Given the average PSNR of all frames, the *Constant quality stage* tries to

encode every frame to reach the average PSNR by adjusting QP. If either of the following two stop conditions is satisfied, the algorithm terminates: a) the difference between the maximal and the minimal PSNR value in a sequence for the quality stage and b) the difference between coded bits and the target bits for the rate stage. In our experiment, the threshold values are 0.5 dB and 2% for the quality stage and the rate stage, respectively. The parameters used by the LCQC algorithm are:  $R_r - R(\lambda)/R_r \leq 0.02$ ,  $\delta_P=0.2$  dB, and  $P_\Delta=P_U-P_L=2$  dB.

As shown in Tables 3.3 and 3.4, typically the LCQC algorithm can match the bit budget very well. The MultiStage algorithm usually has a bit rate mismatch especially at low rates, which are consistent with the report in [27]. The LPF algorithm has a bit rate mismatch too. As discussed in [24], the coding bits converge to the budget bits when the sequence length goes to infinity. Often, the LCQC algorithm has the largest average PSNR and its PSNR variance is controlled at around 0.02 consistently at all rates because the frame quality variation is limited to a range between  $-\delta_P$  and  $\delta_P$ . That is, the PSNR is accurately controlled by adjusting the quality variation parameter. In contrast, the LPF and the MultiStage algorithms try to achieve the constant quality goal only. The LCQC complexity (CPU time) lies in between those of MultiStage and LPF, whereas LPF has the smallest complexity. Both the LCQC and the MultiStage algorithms have a larger complexity at low bit rates due to the large number of iterations for convergence. Fig. 3.3 shows the frame-by-frame PSNR and used bit plots for the *News* and the *Table Tennis* sequences at 64 kbps.



(b)



(d)

Fig.3.3. PSNR and used bit plots of the LCQC, MultiStage, and LPRF algorithms  $P_{\Delta} = 2.0$  dB and  $\delta_p = 0.2$  dB at 64 kbps: (a) PSNR plots for *News* (b) Used bit plots for *News* (c) PSNR plots for *Table Tennis* (d) Used bit plots for *Table Tennis*.

Table 3.3. Comparisons of PSNR, bit rate, and complexity for LCQC, MultiStage, and LPF algorithms on *News* at three bit rates.

Target Rate	Method	Rate(% error)	PSNR(dB)				Time(hr)
			Min	Max	Avg	Var	
24 kbps	LCQC	23.82 (-0.76%)	28.29	29.22	28.57	0.017	2.33
	MultiStage	24.11 (+0.44%)	28.19	28.6	28.36	0.002	3.90
	LPF	23.99 (-0.06%)	28.15	28.62	28.38	0.004	0.41
64 kbps	LCQC	63.93 (-0.11%)	34.35	35.09	34.70	0.018	1.63
	MultiStage	62.49 (-2.36%)	34.35	34.91	34.60	0.006	2.25
	LPF	62.66 (-2.10%)	34.22	34.88	34.54	0.014	0.41
112 kbps	LCQC	111.50 (-0.45%)	37.82	38.61	38.31	0.020	1.17
	MultiStage	107.82 (-3.73%)	37.70	38.45	38.06	0.009	1.42
	LPF	107.19 (-4.30%)	37.70	38.65	38.14	0.021	0.41

Table 3.4. Comparisons of PSNR, bit rate, and complexity for LCQC, MultiStage, and LPF algorithms on *Table Tennis* at three bit rates.

Target Rate	Method	Rate(% error)	PSNR(dB)				Time(hr)
			Min	Max	Avg	Var	
24 kbps	LCQC	23.84 (-0.65%)	26.22	26.84	26.42	0.019	2.33
	MultiStage	25.35 (+5.61%)	26.71	27.31	26.91	0.005	5.94
	LPF	24.31 (+1.29%)	26.18	27.51	26.93	0.018	0.41
64 kbps	LCQC	63.61 (-0.61%)	32.10	33.09	32.48	0.022	2.12
	MultiStage	63.17 (-1.3%)	32.10	32.77	32.47	0.007	3.25
	LPF	62.66 (-2.10%)	32.09	32.79	32.45	0.011	0.41
112 kbps	LCQC	111.65 (-0.31%)	34.92	36.15	35.41	0.028	1.33
	MultiStage	108.76 (-2.89%)	34.92	35.50	35.25	0.007	2.32
	LPF	105.70 (-5.63%)	34.71	35.34	35.01	0.013	0.41

### 3.3.3 Effects of Quality Variation Constraint on PSNR and Complexity

One important feature of our schemes is the flexibility of adjusting the picture quality variation over time. Our schemes achieve the MINAVE goal in (3.1) when  $\delta_P = \infty$ . It produces the constant quality pictures when  $\delta_P$  approaches 0 dB. Generally, if  $\delta_P$  is smaller than 0.4 dB, a consistent quality solution is practically obtained. By adjusting the  $\delta_P$  value in the range of

$[0.4, \infty]$ , we obtain a solution in between the constant quality and the MINAVE.

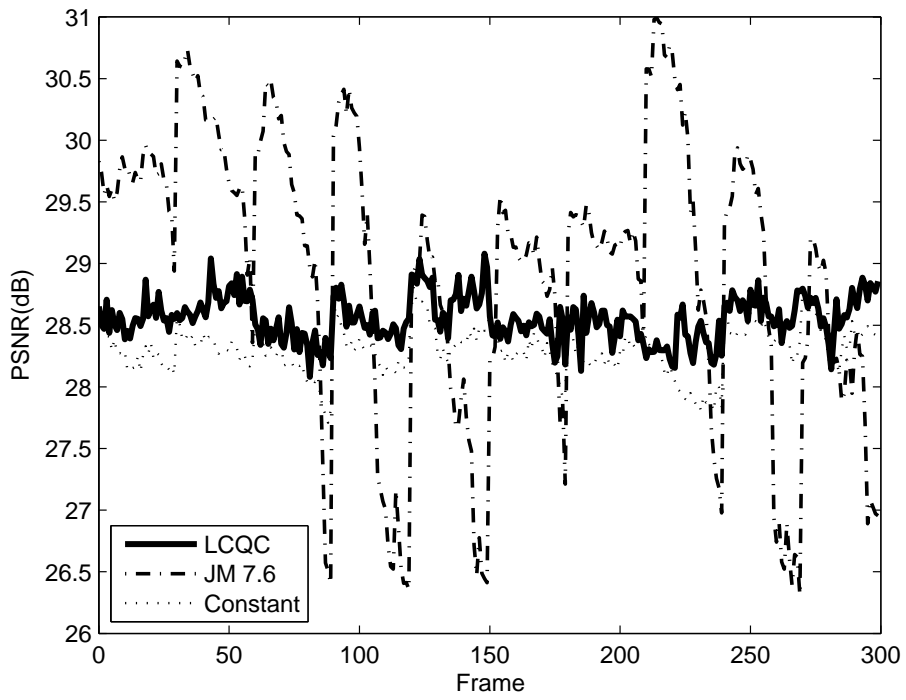
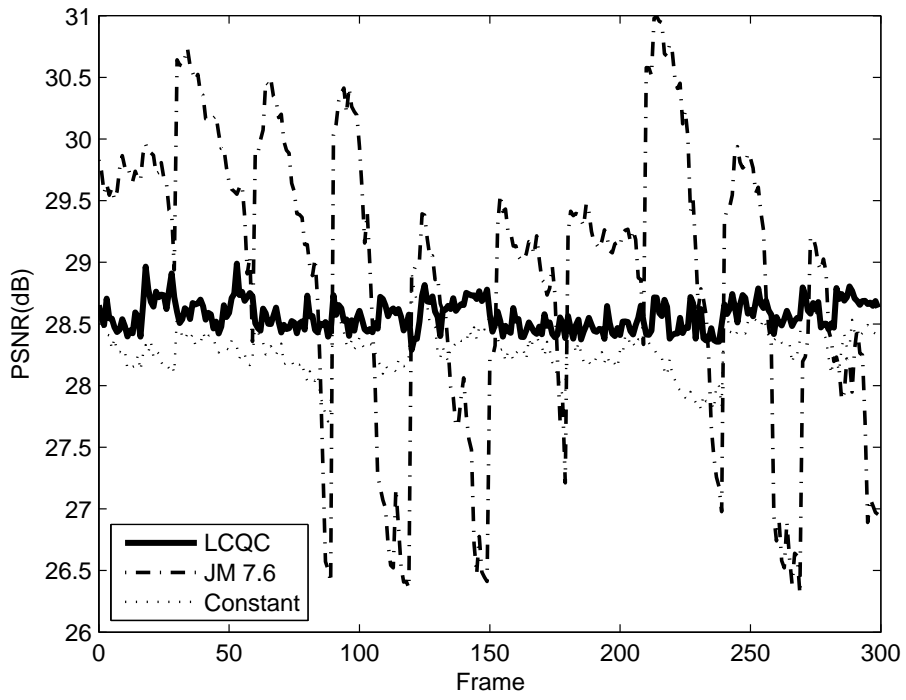
The disadvantage of using a large  $\delta_p$  value is to increase the number of branch expansions and active nodes. It has a much less impact on the LCQC algorithm since LCQC does not have the trellis structure. Table 3.5 shows the test results. Indeed, its computational load increases only slightly from a small  $\delta_p$  to a large  $\delta_p$ .

Table 3.5. Effect of quality variation constraint on PSNR and complexity for the LCQC algorithm on three sequences, Foreman, Table Tennis, and News at three quality constraints.

$$P_{\Delta} = P_U - P_L = 2\text{dB}.$$

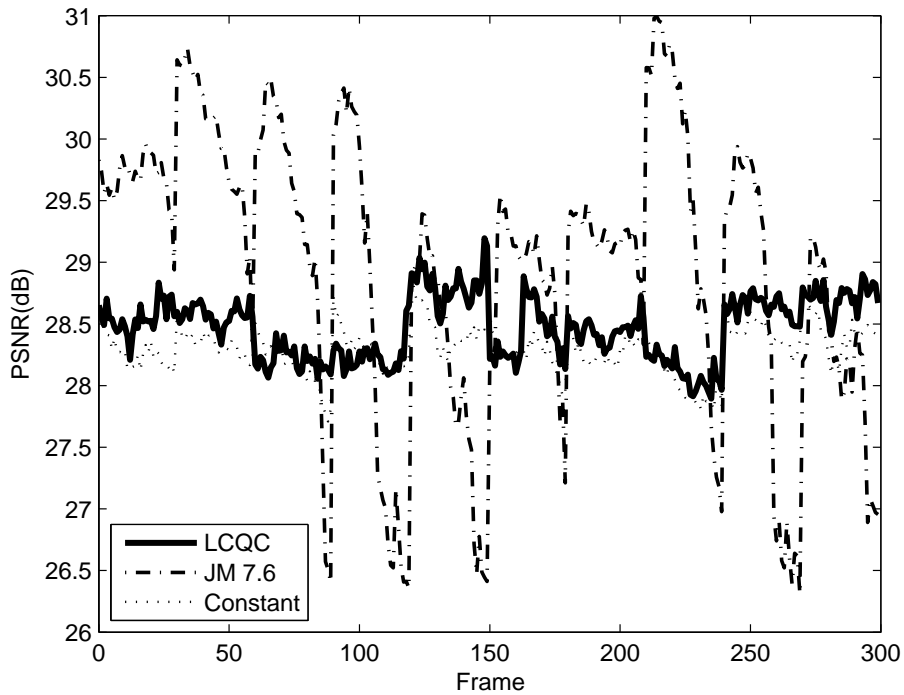
Video	Target Rate	Quality Constraint(dB)	PSNR(dB)				Time(hr)
			Min	Max	Avg	Var	
Foreman	24kbps	0.2	25.76	26.48	26.01	0.017	2.45
		0.4	25.67	26.91	26.07	0.055	2.51
		1.0	25.34	27.48	26.32	0.319	2.56
Table Tennis	64kbps	0.2	32.10	33.09	32.47	0.022	2.12
		0.4	32.09	33.15	32.50	0.049	2.23
		1.0	31.75	33.62	32.81	0.138	2.31
News	112kbps	0.2	37.82	38.61	38.31	0.020	1.17
		0.4	37.75	38.70	38.34	0.027	1.24
		1.0	37.93	39.31	38.47	0.062	1.29

Fig. 3.4 is the frame PSNR plot for the *News* sequence at different quality variation constraints. Simulation results show that a larger  $\delta_p$  value leads to larger picture variation but produces a higher PSNR. As shown in Fig. 3.4(b), the PSNR curve produced by LCQC has little variation at the beginning of the sequence as compared to that of TCQC in Fig. 3.2(a). It shows that the LCQC algorithm generates even more smooth PSNR outputs.



(b)





(c)

Fig.3.4. LCQC results for *News* at 24 kbps and  $P_{\Delta}=2.0\text{dB}$  : (a)  $\delta_P = 0.2\text{dB}$ . (b)  $\delta_P = 0.4\text{dB}$ . (c)  $\delta_P = 1.0\text{dB}$ .

### 3.3.4 Effects of Cluster Size on PSNR and Complexity

Table 3.6 shows the TCQC results at various  $P_{\Delta}$  values. As expected, the average PSNR value decreases when  $P_{\Delta}$  gets larger. The *granularity loss* is defined as the absolute PSNR differences between  $P_{\Delta}=0.1$  dB case (very fine granularity) and the larger  $P_{\Delta}$  cases. When the cluster size is very small ( $P_{\Delta}=0.1$  dB), we essentially achieve the best possible results without PSNR loss due to the use of cluster. As expected, the granularity loss is getting larger as the cluster size is larger than 0.1 dB.

Since LCQC does not have trellis structure, LCQC has no granularity loss. But on the other hand, the LCQC formulation is an approximation to the integer programming problem [11]. Also, in the lambda search procedure, we stop at a given tolerance. Therefore, there is a performance loss due to the use of Lagrange cost and tolerance. Table 3.7 shows the test results of TCQC and LCQC at the same quality variation of  $\delta_P=0.4\text{dB}$  and the same PSNR

range of  $P_U - P_L = 2\text{dB}$ . The cluster size is 0.1 dB for TCQC. As expected, TCQC is slightly better but the PSNR difference is typically less than 0.3 dB. Again, LCQC is much faster in speed.

Table 3.6. Effect of cluster size  $P_\Delta$  on the PSNR loss for the TCQC algorithm on *Foreman* and *Table Tennis* at three cluster sizes and  $\delta_P = 0.4$  dB.

Video	Target Rate	Cluster Size (dB)	PSNR(dB)	
			Avg	Granularity Loss
Foreman	112 kbps	0.1	35.38	0.00
		0.2	35.29	0.09
		0.4	35.01	0.37
Table Tennis	24 kbps	0.1	26.74	0.00
		0.2	26.73	0.01
		0.4	26.62	0.12

Table 3.7. Comparisons of average PSNR, bit rate, and complexity in TCQC and LCQC algorithms for three sequences.

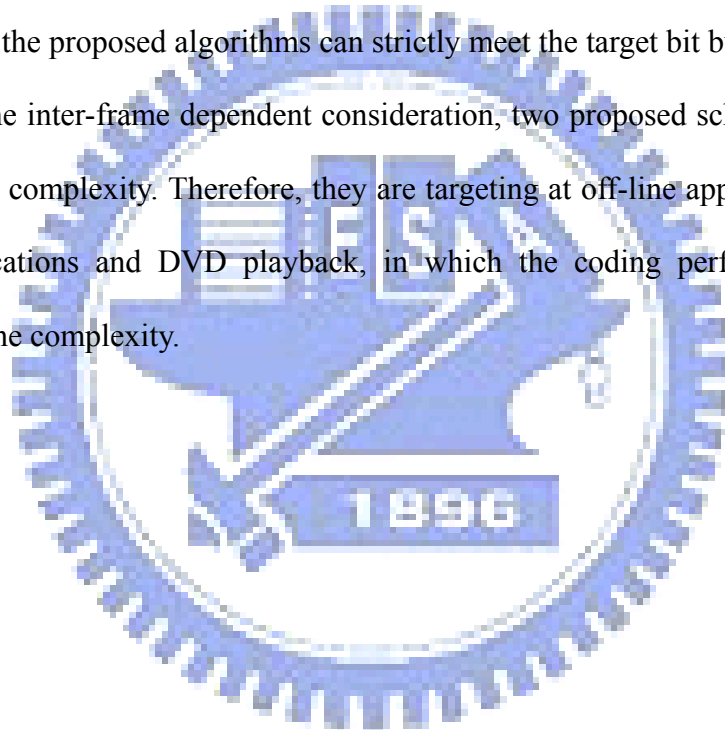
Video	Target Rate	Rate(% error)		Avg. PSNR(dB)		Time(hr)	
		TCQC	LCQC	TCQC	LCQC	TCQC	LCQC
Foreman	24 kbps	23.83 (-0.73%)	23.69 (-1.30%)	26.11	26.07	8.15	2.51
	64 kbps	63.38 (-0.97%)	63.74 (-0.41%)	32.30	32.30	4.08	1.82
	112 kbps	111.46 (-0.48%)	111.87 (-0.11%)	35.38	35.38	3.21	1.39
News	24 kbps	23.95 (-0.20%)	23.90 (-0.42%)	28.81	28.55	7.56	2.42
	64 kbps	62.95 (-1.65%)	63.23 (-1.20%)	34.81	34.68	3.53	1.69
	112 kbps	109.71 (-4.24%)	111.57 (-0.38%)	38.41	38.34	1.84	1.24
Table Tennis	24 kbps	23.70 (-1.25%)	22.97 (-4.28%)	26.74	26.38	7.98	2.47
	64 kbps	63.17 (-1.30%)	63.68 (-0.51%)	32.61	32.50	5.26	2.33
	112 kbps	111.66 (-0.30%)	111.53 (-0.42%)	35.4	35.37	3.29	1.41

### 3.4 Summary

In this chapter, we realize the triple goal of producing consistent quality videos, minimizing the total distortion and meeting the bit budget strictly. Moreover, this framework can flexibly provide a solution in between the MINAVE and constant quality extremes. Two algorithms are proposed to find the optimal and consistent quality solution. Inspired by the previous work, a trellis-based quality control scheme is firstly proposed. This approach provides a nearly

optimal solution (the resulting total distortion is minimized) for a given bit rate budget on a dependent coding platform. The second algorithm is developed based on the Lagrange multipliers method. We impose the consistent quality constraint on this formulation and also we design a fast procedure to find the optimal solution. As compared to the trellis-based algorithm, it runs much faster and has a performance very close to the former. Simulation results show that both approaches have the largest PSNR average at a slight PSNR variation as compared to the other published consistent quality proposals and have a much smaller PSNR variation at a slight average PSNR loss as compared to the MPEG JM rate control. In addition, only the proposed algorithms can strictly meet the target bit budget requirement.

Due to the inter-frame dependent consideration, two proposed schemes have rather high computational complexity. Therefore, they are targeting at off-line applications such as video storage applications and DVD playback, in which the coding performance has a higher priority than the complexity.



# Chapter 4

## Graceful Quality Control Algorithm

In this chapter we discuss the graceful quality variation target needed for the video transmission applications. Since the channel capacity is time-varying, the channel estimation is usually employed to predict the available channel bit rate per GOP duration. Or, equivalently, the GOP budget bits vary over time. This circumstance creates the needs that the coded picture quality shall gradually change to match the fluctuation of the channel bit rate. Due to lower complexity needed in transmission applications, we use the Lagrange-based method only. In Section 4.1, the graceful quality variation problem is formulated mathematically. In Section 4.2, the proposed LCQC algorithm is modified and employed to achieve the graceful quality variation goal for its simplicity and efficient. Section 4.3 presents the simulation results which show the effectiveness of our algorithm for video transmission applications. Section 4.4 summarizes the findings and their limitations.

### 4.1 Graceful Quality Variation Problem

Inter-frame quality control is necessary in achieving the smooth video representation. Because the proposed quality coding scheme controls picture quality inside a GOP, the quality control across GOP boundaries is also needed. As discussed in Section 3.1.2, it is clear that using distortion, not the bit rate, is more convenient to achieve the graceful quality variation. That is, we also use the proposed proposition in Section 3.1.2 to perform  $MinR(D_T)$  rather than  $MinD(R_T)$  except that the coding performance is evaluated on the GOP basis instead of on the sequence basis. This problem is thus formulated as follows.

In the independent coding formulation, the  $k$ th frame distortion and bits in a GOP, i.e.,  $d_k$  and  $r_k$ , only depend on the current frame QP values. Given  $K$  frames in a GOP and a total GOP bit budget  $R_T$ , our goal is to minimize the overall GOP distortion  $D$  by choosing the optimal frame-level QP values  $\mathbf{q}^* = \{ q_0^*, q_1^*, q_2^*, \dots, q_{K-1}^* \}$  for all  $K$  frames, where  $q_k^* \in Q$ , for  $k=0,1,\dots,K-1$ . That is,

$$\mathbf{q}^* = \arg \min_{q_k \in Q} D = \sum_{k=0}^{K-1} d_k(q_k),$$

subject to the constraints

$$R = \sum_{k=0}^{K-1} r_k(q_k) \leq R_T, \text{ and} \quad (4.1)$$

$$|f(d_k) - f(d_{k-1})| \leq \delta_p, \forall k \in \{0, 1, \dots, K-1\},$$

where  $f(\cdot)$  is the PSNR function calculated by  $f(d) = 10 \log_{10}(255^2 \times FPN/d)$  and  $FPN$  is the pixel number in a frame. The second constraint in (4.1) is added to limit the inter-frame quality variation; that is, the difference PSNR is limited by  $\pm \delta_p$ . In addition, to consider the quality control across GOP boundaries, the quality constraint on the first frame in a GOP can be specified by the last frame in the previous GOP, except for the first GOP. More specifically, the first frame quality  $f(d_0)$  in a GOP is limited by the last frame quality  $f(d_{-1})$  in the previous GOP.

## 4.2 Graceful Quality Control Algorithm

In this Section, we propose to use the Lagrange-based method to solve the inter-frame quality variation problem. As shown in Section 3.2.4, the Lagrange-based LCQC method is introduced to solve the consistent quality problem across all frames in a sequence. Simulation results show that the Lagrange-based method has a lower computational complexity and its PSNR value is on a par with that of the Trellis-based method when the optimal lambda value

is found. Therefore, the proposed LCQC algorithm is modified to meet the need of graceful quality change in the transmission applications and a new Lagrange-based graceful quality control (LGQC) method is thus developed.

The LGQC algorithm differs from the LCQC algorithm in that the quality constraint is imposed on the neighboring frame and each GOP is independently processed. The current frame quality  $f(d_k)$  limited by  $f(\bar{D}) \pm \delta_p$  in (3.1) is replaced with  $f(d_{k-1}) \pm \delta_p$  in (4.1) even when the GOP boundary is crossed. Since each GOP is independently processed, the optimal lambda value of each GOP can be different. Further, the optimal lambda search complexity can be reduced by referring to the optimal lambda value in the previous GOP. In addition, the consistent quality constraint, i.e.,  $P_L \leq f(\bar{D}) \leq P_U$ , is no longer needed in the graceful quality control applications. The LGQC procedure is described as follows.

First, the budget constraint of  $R(\lambda^*) = R_T$  is relaxed. We start with two initial lambda values,  $\lambda_U$  and  $\lambda_L$ , such that  $R(\lambda_U) < R_T < R(\lambda_L)$  is satisfied. We then find a proper lambda range, denoted by  $[\lambda_{LL}, \lambda_{UU}]$ , which includes the lambda value as a part of the solution to the  $\text{Min } J(\lambda)$  problem with two constraints,  $|f(d_k) - f(d_{k-1})| \leq \delta_p$ , and  $R(\lambda_{UU}) < R_T < R(\lambda_{LL})$ . Thus, the optimal lambda value  $\lambda^*$  is guaranteed to locate in the selected range. Then, we employ a fast bisection algorithm to find the optimal solution to the  $R(\lambda^*) = R_T$  problem. The lambda search process iterates until the predefined bit rate tolerance, i.e.,  $R_T - R(\lambda)/R_T \leq \varepsilon$ , is satisfied. After the first GOP is done, we set the next initial lambda interval  $[\lambda_L, \lambda_U]$  with  $[0.2\lambda^*, 5\lambda^*]$  empirically to reduce the search complexity for the optimal lambda value  $\lambda^*$  in the next GOP. Overall, the step-by-step LGQC algorithm is summarized below.

---

*Algorithm 3: Lagrange-based Graceful Quality Control (LGQC) Algorithm*

---

Step0: Start with two values  $\lambda_u$  and  $\lambda_l$  such that  $R(\lambda_u) < R_T < R(\lambda_l)$ . Set  $\lambda_r = (\lambda_l + \lambda_u)/2$  and frame index  $k=0$ .

Step1: Given  $\lambda_r$ , use the fast branch expansion technique to examine all the QPs that satisfy  $|f(d_k) - f(d_{k-1})| \leq \delta_p$ .

Step2: Encode the current frame again using the current QP value. If the current frame is not the last frame in the GOP, let  $k = k+1$ , go to Step 1.

Step3: If  $R(\lambda_r) < R_T$  set  $\lambda_{uu} = \lambda_u = \lambda_r$ . Else set  $\lambda_{ll} = \lambda_l = \lambda_r$ . If the lambda interval boundaries,  $\lambda_{ll}$  and  $\lambda_{uu}$ , are both found, go to Step 4. Otherwise, let  $\lambda_r = (\lambda_l + \lambda_u)/2$ ,  $k = 0$ , go to Step 1.

Step4: Perform the fast bisection search algorithm [30] in the lambda range  $[\lambda_{ll}, \lambda_{uu}]$  to find the optimal  $\lambda^*$ , i.e.,  $R(\lambda^*) = R_T$ . The usual stop rule  $|R_T - R(\lambda)|/R_T \leq \varepsilon$  is adopted. A few assistant techniques are proposed in [30] so that this search process converges rather fast. Normally, this step takes 2 to 4 iterations. The final  $\lambda^*$  and its associated QPs are our optimal solution. This GOP is now done. Go to Step 2 and set  $\lambda_r = \lambda^*$ ,  $\lambda_l = 0.2 \times \lambda^*$ ,  $\lambda_u = 5 \times \lambda^*$ , and the frame index  $k=0$ , if we continue encoding the next GOP.

### 4.3 Simulation Results

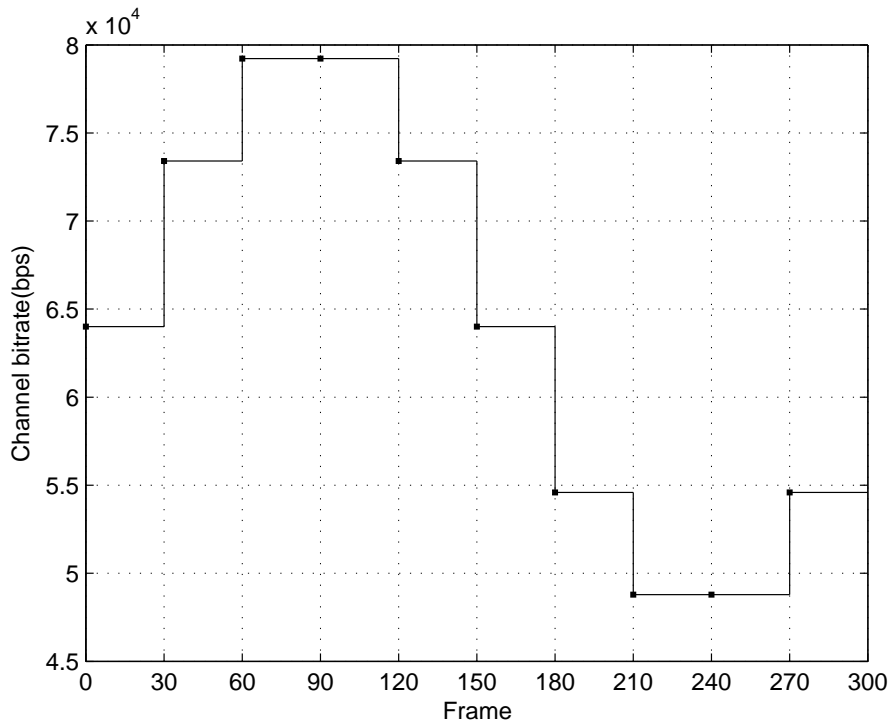
We have implemented the proposed graceful quality control algorithm on the MPEG-4 AVC/H.264 video coder with the RDO option turned on. Its performance is evaluated using two standard MPEG video sequences, *Foreman* and *Carphone*. All test videos are 300 frames in QCIF size. The GOP size is 30. Only I- and P- frames are in use. The channel bit rate for

each GOP is set to follow the sinusoidal fluctuation patterns. Simulations are performed on a 3-GHz Intel Pentium CPU.

We conduct two sets of simulations to evaluate the proposed LGQC algorithm. First, the PSNR performance of the LGQC algorithm is compared to that of JM7.6 rate control at the varying channel bit rate and the first QP in the JM7.6 rate control is set to be identical to that of the LGQC algorithm. Next, the PSNR and complexity of the LGQC algorithm are compared with two inter-frame quality variation values  $\delta_P$  to show the PSNR and complexity tradeoff. Because we use only the Lagrange-based method, the analysis of cluster size effect is not needed.

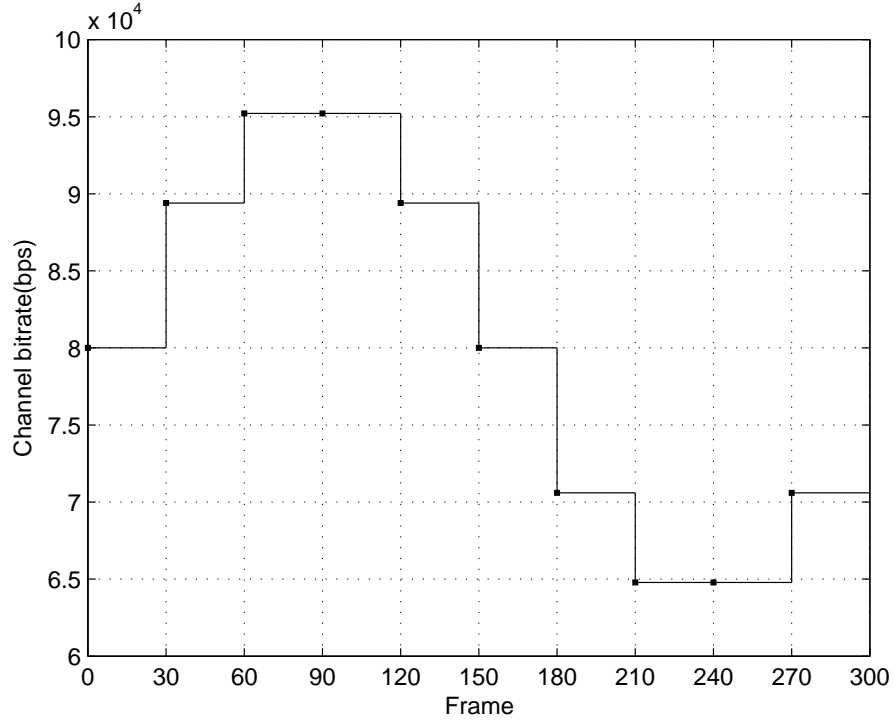
### 4.3.1 LGQC Performance Comparison with JM

The LGQC algorithm is evaluated on two different video sequences, *Foreman* and *Carphone*, at two time-varying GOP bit rate sets. Their bitrate variations follow the stairstep patterns shown in Figs. 4.1(a) and 4.1(b) respectively.



(a)



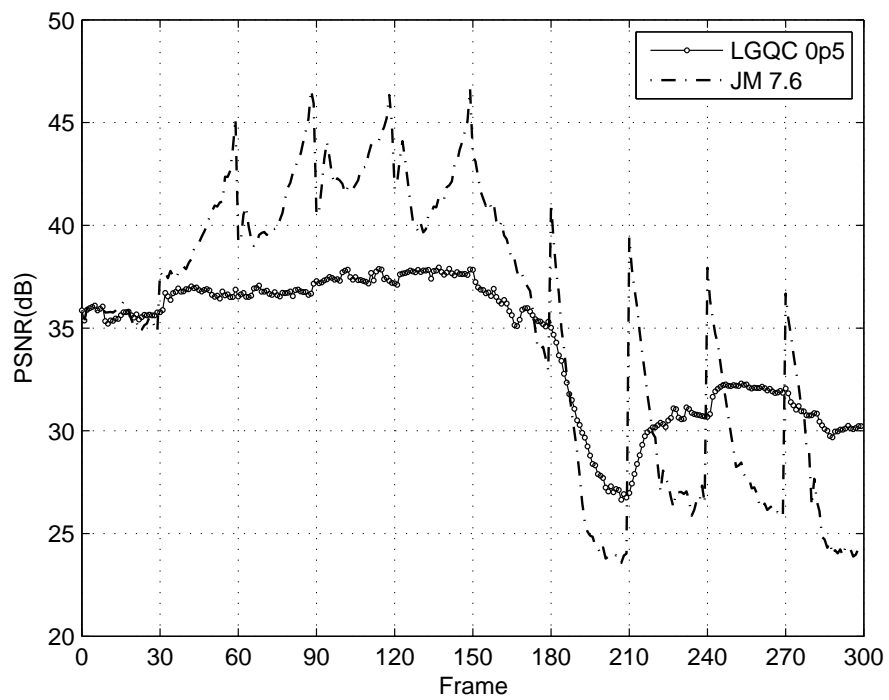
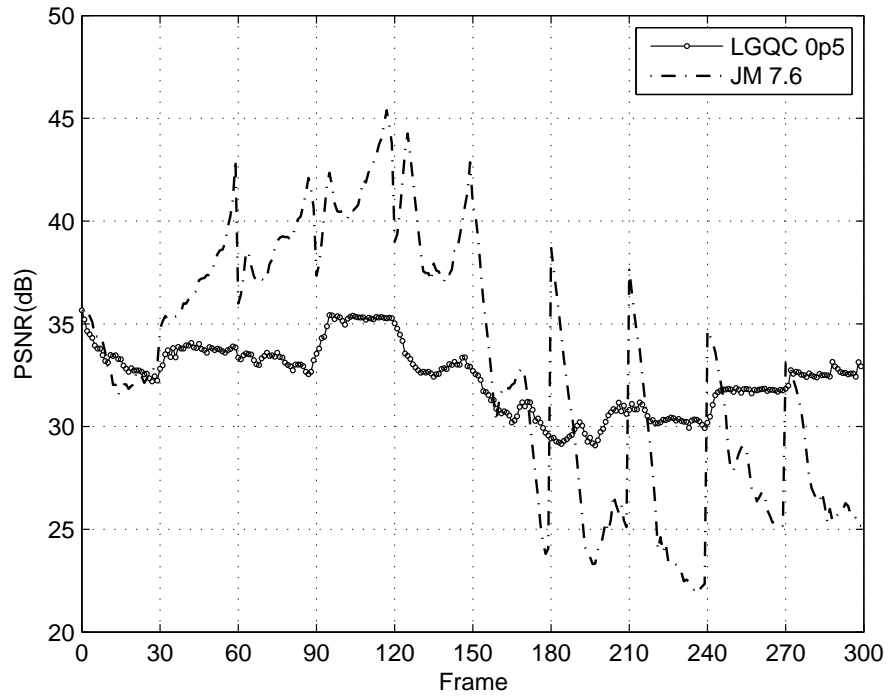


(b)

Fig.4.1. Channel bit rate patterns for LGQC graceful quality control test on two different video sequences. (a) *Foreman*, and (b) *Carphone*.

Fig. 4.2 depicts the frame-by-frame PSNR plots for LGQC and JM7.6 algorithms at two varying channel bit rates. The maximal quality variation parameter used in the LGQC algorithm is  $\delta_p=0.5$  dB. The LGQC PSNR curve has no drop at the GOP boundaries. It has a smoother shape at the largely varying channel bit rate as compared to that of JM7.6. Obviously, the PSNR variance of JM7.6 is very large. This is because the first QP in the current GOP is upper and lower bounded by that in the previous GOP. The average PSNR values of JM 7.6 and LGQC are 33.27 dB and 32.40 dB in Fig. 4.2(a) and 35.42 dB and 34.26 dB in Fig. 4.2(b) respectively. However, the JM algorithm has a large bit rate mismatch. The budget bit achievement ratio of JM 7.6 is 205.54% in Fig. 4.2(a) and 184.66% in Fig. 4.2(b) respectively. In contrast, the budget bit achievement ratio of LGQC is 99.81% in Fig. 4.2(a) and 99.75% in Fig. 4.2(b) respectively. Thus, the proposed Lagrange-based method achieves

nearly the optimal solution. Although the JM 7.6 PSNR performance is better but it uses a much higher bitrate and it has a large swing of more than 20 dB in PSNR across the entire sequence. We summarize these simulation results in Table 4.1.



(b)

Fig.4.2. PSNR plots of the LGQC and JM7.6 algorithms for two sequences at two different channel bit rates. (a) Foreman sequence using rate pattern in Fig. 4.1(a). (b) Carphone sequence using rate pattern in at Fig. 4.1(b).

Table 4.1. Comparisons of PSNR, bit rate, and complexity for JM 7.6 and LGQC algorithms on the *Foreman* and *Carphone* sequences at two varying channel bit rates.

Video	Avg Target Bit Rate	Method	Rate(% error)	PSNR (dB)				Time(hr)
				Min	Max	Avg	Var	
Foreman	64 kbps (Fig. 4.1(a))	JM7.6	131.55 (+105.54%)	22.06	45.39	33.27	38.04	0.13
		LGQC at $\delta_p = 0.5\text{dB}$	63.88(-0.19%)	29.09	35.66	32.40	2.68	1.42
		LGQC at $\delta_p = 1.0\text{dB}$	63.96 (-0.06%)	28.63	35.42	32.40	2.54	1.53
Carphone	80 kbps (Fig. 4.1(b))	JM 7.6	147.73 (+84.66%)	23.57	46.64	35.42	44.97	0.13
		LGQC at $\delta_p = 0.5\text{dB}$	79.80(-0.25%)	26.65	37.95	34.26	10.58	1.65
		LGQC at $\delta_p = 1.0\text{dB}$	79.94 (-0.08%)	28.99	37.93	34.35	9.43	1.87

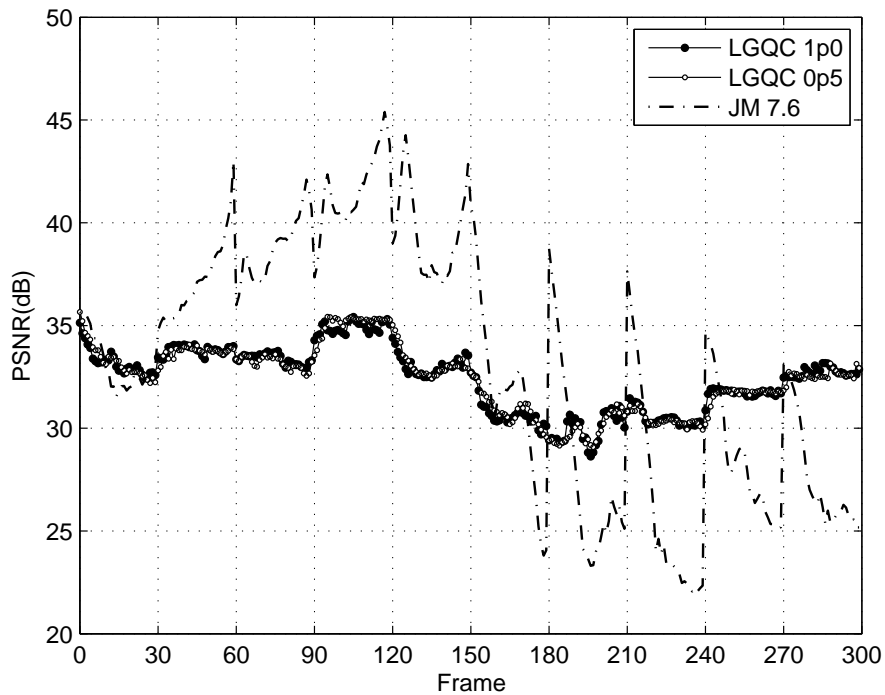
### 4.3.2 Effects of Quality Variation Constraint on PSNR and Complexity

In this section, we change the quality variation parameter  $\delta_p=1.0\text{dB}$  and rerun the experiments in Section 4.3.1. We like to see the effect of quality variation constraints on PSNR and complexity. Fig. 4.3 is the frame PSNR and used bit plots for *Foreman* and *Carphone* sequences at two  $\delta_p$  values. The details of numerical values are shown in Table 4.1.

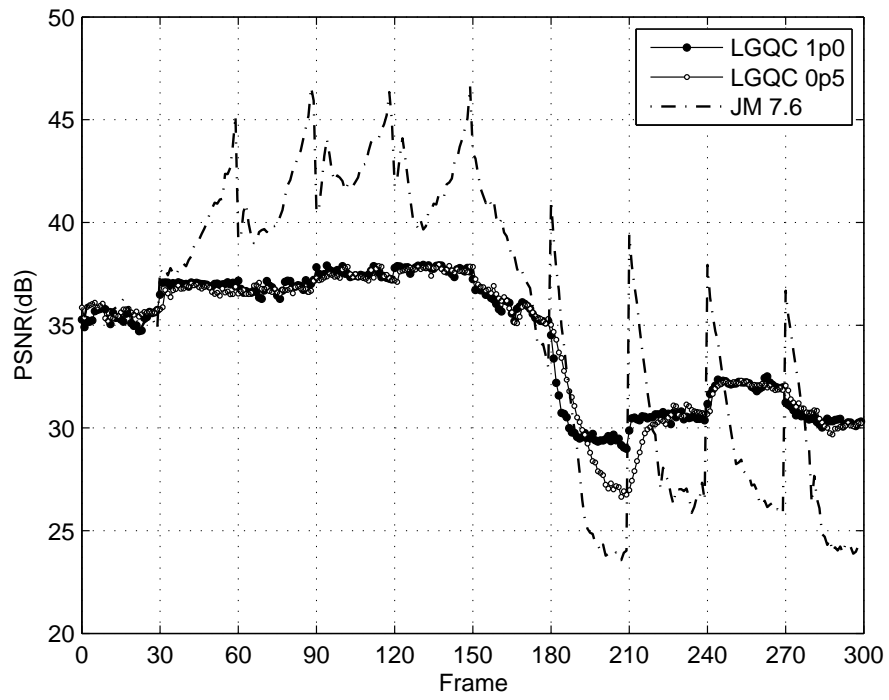
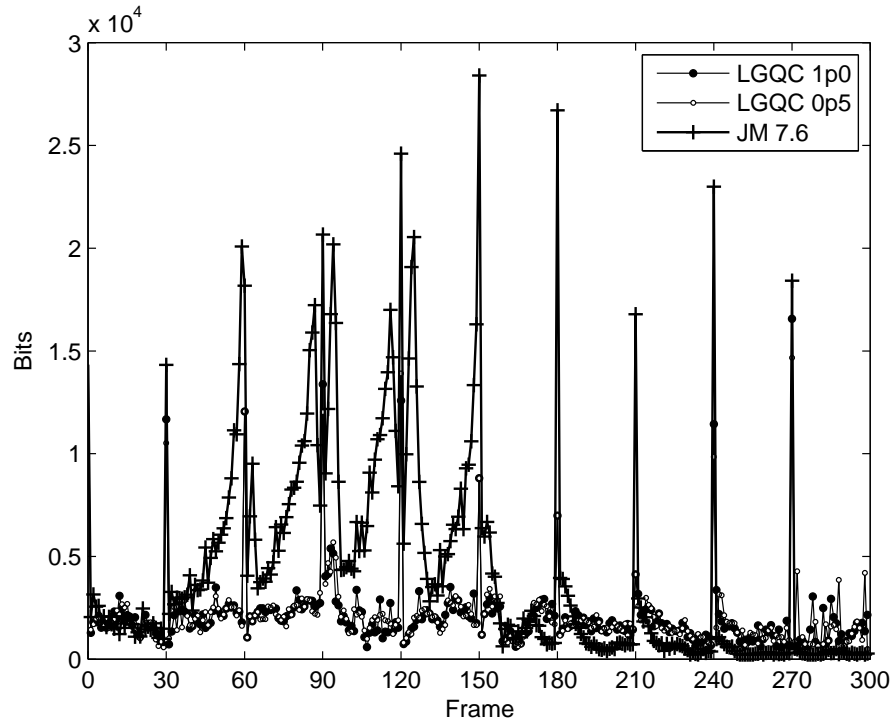
As shown in Fig. 4.3(a) for the *Foreman* sequence, the PSNR curve produced by the  $\delta_p=1.0\text{dB}$  case has similar frame-by-frame quality variation as compared to that of  $\delta_p=0.5\text{dB}$  case. It indicates that the quality constraint of  $\delta_p=0.5\text{dB}$  is sufficient to achieve the optimal solution for the *Foreman* sequence at the given GOP budget bits. Note that  $\delta_p$  is defined by the “maximal” quality variation allowed between two nearby frames. In contrast, the simulation results in Fig. 4.3(b) for the *Carphone* sequence show similar results except for the frames between 180 and 210, where the scene change occurs. It show that  $\delta_p=0.5\text{dB}$  has a

large quality variation in this GOP. As stated in Section 3.3.3, a larger  $\delta_p$  value leads to a larger picture variation but produces a higher PSNR. This claim has an implicit assumption that a larger bitrate is available in these frames which contain high motion or scene changes. Due to the limited GOP budget bits (the number of frames is small) and the imposed inter-frame quality variation constraint, a good bit allocation policy applied to scene change is to decrease the frame quality as early as possible. Therefore, the quality variation of the  $\delta_p=1.0\text{dB}$  case is smaller than that of the  $\delta_p=0.5\text{dB}$  case during this scene change period. As shown in Table 4.1, the minimum PSNR values are 28.99 dB and 26.65 dB for LGQC  $\delta_p=1.0\text{dB}$  and  $\delta_p=0.5\text{dB}$  cases, respectively. Consequently, a larger  $\delta_p$  case produces a higher average PSNR.

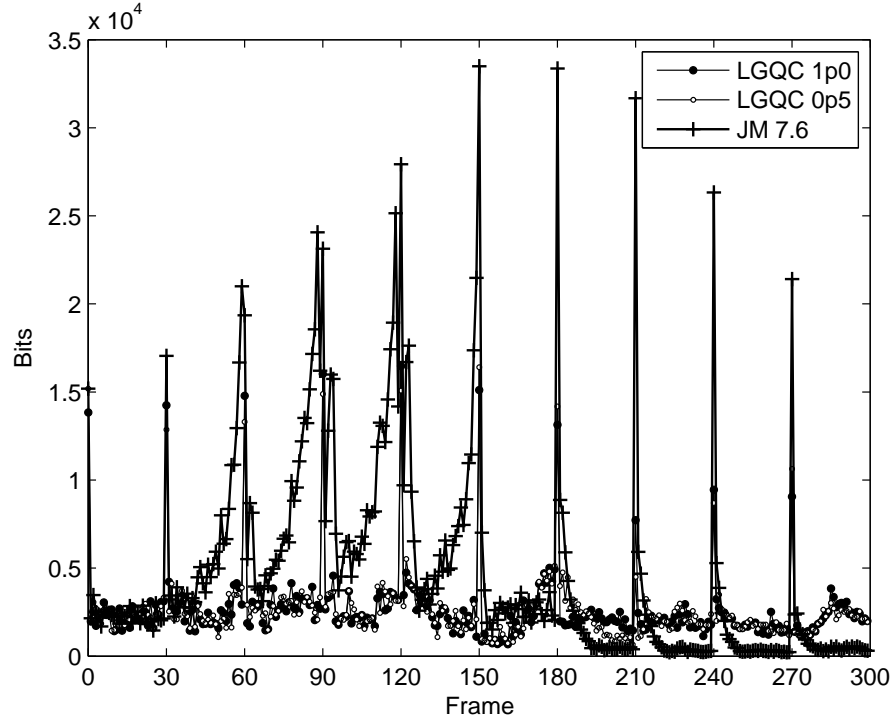
Clearly, using a large  $\delta_p$  value shall increase the number of branch expansions. However, because the proposed LGQC algorithm uses the fast branch expansion process introduced in Section 3.2.3, the computational load increases only slightly. As shown in Table 4.1, the increased computation is around 0.1 hour.



(a)



(c)



(d)

Fig.4.3. PSNR and used bit plots of the LGQC with two  $\delta_P$  values and JM7.6 algorithms for two sequences at two different channel bit rates. (a) Foreman sequence PSNR plots at Fig. 4.1(a) bit rate. (b) Foreman sequence used bit plots at Fig. 4.1(a) bit rate. (c) Carphone sequence PSNR plots at Fig. 4.1(b) bit rate. (d) Carphone sequence used bit plots at Fig. 4.1(b) bit rate.

## 4.4 Summary

In this chapter, we aim at the smooth video representation for time-varying channels and the total distortion is minimized and the bit budget is met accurately. The third algorithm is proposed to find the optimal solution to solve this problem. First, the problem is formulated mathematically. Next the step-by-step procedures are described and verified by simulation. It is shown that the proposed algorithm yields smoother video quality than the JM7.6 rate control and the total bits used are very close to the given budget bits. In addition, the effect of quality variation parameters on PSNR and complexity is discussed.

Despite the optimality of proposed method in this chapter, their computational load is still high. Vector or parallel processing hardware structure is needed for its real-time implementation. Thus, the proposed algorithm may be more suitable for off-line applications such as Internet video streaming.



# Chapter 5

## Conclusions and Future Research Topics

In this thesis, we discuss the consistent and graceful quality control techniques for video storage and transmission applications. The main results of the thesis are summarized below.

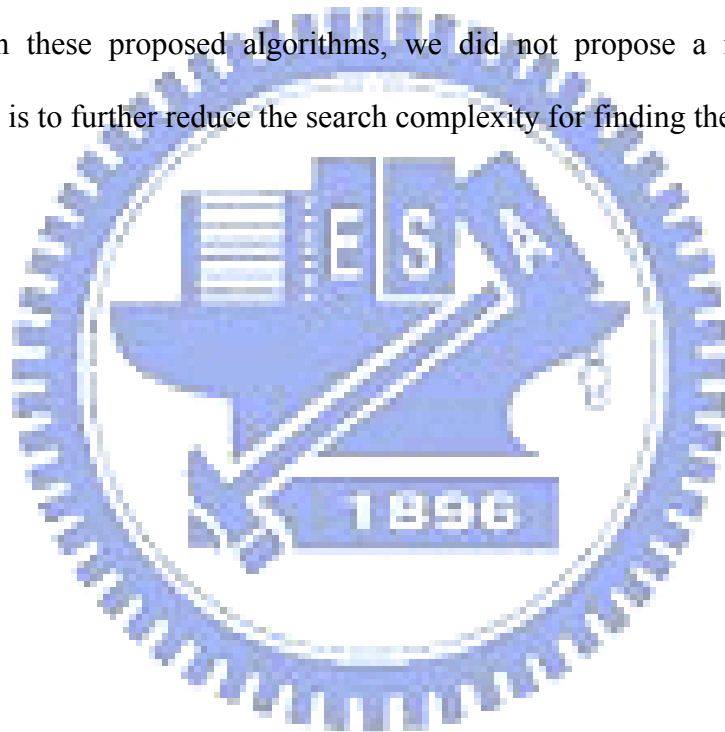
The study of consistent quality control technique is discussed in Chapter 3. Many existing schemes cannot achieve at the same time the goal of minimizing total distortion and the goal of meeting budget bits accurately for constant quality representation. In contrast, this study achieves three goals (a) consistent video quality (b) minimizing the total distortion and (c) meeting the bit budget accurately. Moreover, by adjusting one key parameter, the goal in the proposed framework can also be the constant quality or the MINAVE quality. Two algorithms are proposed to find the optimal and consistent quality solution. A trellis-based quality control scheme is firstly proposed. Then the Lagrange multipliers method with fast branch expansion process and optimization procedure is proposed to significantly reduce the computational complexity at a slight average PSNR loss. Simulation results show that both approaches have the largest average PSNR at a slight PSNR variation as compared to the other existing consistent quality proposals and they have a much smaller PSNR variation at a slight average PSNR loss as compared to the MPEG JM rate control. In addition, only the proposed algorithms can strictly meet the target bit budget requirement.

The Lagrange multipliers method is attractive for its simplicity and efficiency in the consistent quality applications. In Chapter 4, we discuss the graceful quality fluctuation needed in source encoding to accommodate the time-varying channel bandwidth. Due to lower complexity needed in transmission applications, we use the Lagrange-based method



only. Based on the second algorithm, the third algorithm is proposed to achieve the graceful quality variation goal while minimizing the total distortion and meeting the bit budget accurately. Simulation results show that the proposed algorithm produces smoother quality videos and the total bits used are very close to the given budget bits.

In this thesis, we discuss the design and analysis of a quality control framework in video coding. Some potential research topics are as follows. First, the joint source-channel coding is not discussed but it is an important topic. In Appendix A, our study related to channel coding is presented for future source-channel integration. Second, although the optimal performance is achieved in these proposed algorithms, we did not propose a real-time algorithm. A potential topic is to further reduce the search complexity for finding the optimal lambda value.



# Appendix A

## Performance Analysis for Serially

## Concatenated FEC in IEEE802.16a over

## Wireless Channels

### A.1 Introduction

Recently, IEEE has proposed the standard referred to as IEEE802.16a for the local and metropolitan area network [39]. Its serially concatenated FEC scheme consists of an RS(255,239,8) code as the outer code and RCPC codes as the inner code.

To combat the severe channel degradation, concatenating RS code with convolutional code (CC) could enhance their error control performance [40]. One advantage of using RS/RCPC concatenated codes is that they can provide multiple services and multiple rate transmissions, which is particularly useful for multimedia communications.

The idea of RCPC codes was first introduced by Hagenauer [37]. The performance analysis of this type of codes over wireless channels could be found in [41]. However, few studies have been reported on the performance analysis of the concatenation of the RS code and the RCPC codes together. In addition, we like to identify a suitable operational range in terms of signal-to-noise ratio and acceptable performance. The aim of this appendix is to investigate the performance of RS/RCPC concatenation defined by the IEEE802.16a specifications over the AWGN and the FI-RFC channels [41]. We derive the union upper bounds on the BPSK-modulated BER (bit-error-rate) at the output of the concatenated RCPC

and RS code. Also, we compare the theoretical bounds with the simulation results.

The rest of this appendix is organized as follows. Section A.2 describes the system model. Union upper bounds on BER and PER are derived in Section A.3. Section A.4 shows the simulation results and comparisons are made with the theoretical upper bound. Finally, conclusions are drawn in Section A.5.

## A.2 System Model

The model of the transmission system to be analyzed is shown in Fig. A.1. The message bit stream in the analysis and simulation is assumed to be a random bit sequence  $u_i$ . The message bits are packed into blocks of  $239 \times 8$  bits since the RS code operates over  $GF(2^8)$ . Each block is first coded by RS(255,239,8) coder. This coder inserts  $16 \times 8$ -bit redundancies for each block. Thus, the output is a packet of length 255 bytes, which are then fed into the RCPC coder. The mother code of this RCPC code has a coding rate of  $1/2$  and a constraint length of 7. With different puncture patterns (perforation matrices), this RCPC is capable of producing five different coding rates:  $1/2$ ,  $2/3$ ,  $3/4$ ,  $5/6$ , and  $7/8$ . Therefore, depending on the channel condition, we can select an appropriate bit rate that leads to the best trade-off between data throughput and error probability. A number of tailing bits are inserted to ensure proper decoding operation with an acceptable decoding delay. The choice of tailing bits leads to a tradeoff between the error control performance and the data throughput rate. Another parameter in the practical Viterbi decoding process is the decoder depth (decision path length). This study uses 10 tailing bits and the decoder depth is 210 bits, 35 times the memory span of the mother convolutional code of the given RCPC to get better performance in the Rayleigh fading channel. The coded bits are the BPSK-modulated and the modulated symbols  $\{x_i\}$  are transmitted.

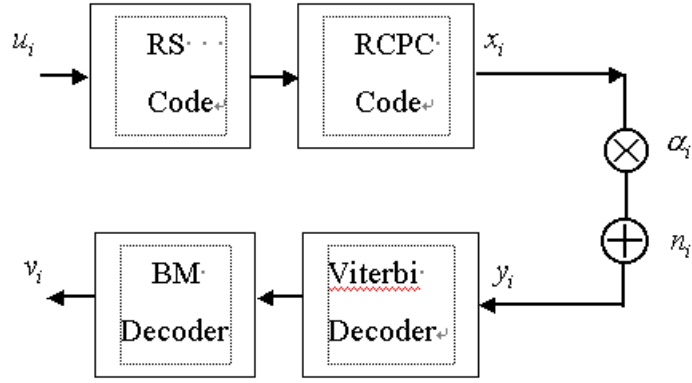


Fig. A.1. System model.

Suppose the test channel has slow and flat Rayleigh fading, then the phase error can be perfectly tracked. We further assume coherent demodulation is available. The received sample  $y_i$  is thus expressed in the form

$$y_i = \sqrt{\frac{2R_c E_b}{N_0}} \alpha_i x_i + n_i \quad (\text{A.1})$$

where  $E_b$  is the energy per information bit,  $R_c$  is the selected code rate of RCPC codes, and  $n_i$  is the zero mean white Gaussian noise sample with unit variance. Because we assume the channel is a fully interleaved Rayleigh fading channel, the sequence  $\{\alpha_i\}$  of the fading envelope is independent and is identically Rayleigh distributed with the following probability density function,

$$f(\alpha) = \frac{\alpha}{\sigma^2} e^{-\frac{\alpha^2}{2\sigma^2}} \quad (\text{A.2})$$

where  $\sigma^2$  is the time-average power of the received signal before the envelop detection and the fading envelope  $\alpha$  has the properties of  $\alpha \geq 0$  and  $E[\alpha^2] = 1$ . Moreover,  $\alpha$  is set to one for the AWGN channel. Soft decision decoding (SDD) with no quantization is used in conjunction with the Viterbi decoding process. In the RS decoding, the Berlekamp-Massey based algorithm is used in simulation and only the error-correction ability is considered. After RS decoding, the output bit sequence  $\{v_i\}$  is obtained and then the BER (bit error rate) and

PER (packet error rate) of the RS code are calculated.

## A.3 Performance of Serially Concatenated FEC

In this section, the upper bounds on BER and PER of serially concatenated FEC are derived for the AWGN and the FI-RFC channels. In the IEEE802.16a specifications, the concatenated FEC can operate together with both BPSK and QPSK modulations; however, we analyze the BPSK modulated signal only, since the performance of QPSK modulation is essentially the same as that of BPSK [43].

### A.3.1 Union Upper Bound on the BER of RCPC Codes

The typical union bound can be expressed in the form

$$P_{b,RCPC} \leq \frac{1}{pp} \sum_{d=d_f}^{\infty} c_d \times p_2(d) \quad (\text{A.3})$$

where  $pp$ ,  $d_f$ , and  $c_d$  are the puncture period, free distance, and weight distribution coefficient, respectively. Detailed description of the above parameters can be found in [42]. Here, we calculate upper bound of  $P_{b,RCPC}$  by summing up the Hamming distance  $d$  in the range of  $d_f$  to  $d_f + 9$ . Without loss of generality, transmission of the all-zero sequence is assumed and the pair-wise error probability  $p_2(d)$  is referred to the case of selecting an incorrect path with Hamming weight  $d$  in the Viterbi decoding process. In AWGN and coherent BPSK scheme,  $p_2(d)$  is given by

$$P_2(d) = Q\left(\sqrt{\frac{2dR_c E_b}{N_0}}\right) \quad (\text{A.4})$$

where the  $Q$  function is defined by  $Q(x) = (\sqrt{2\pi})^{-1} \int_x^{\infty} e^{-x^2/2} dx$ . Under the FI-RFC, coherent BPSK, SDD, and perfect channel estimates  $\{\alpha_i\}$  assumptions, the pair-wise error rate  $p_2(d)$  is derived using the concept of diversity. The concatenated FEC utilizes the time diversity technique to attain independent fading envelope  $\alpha_i$  among the received coded symbols. A

closed form of the pair-wise error rate  $p_2(d)$  is given by

$$P_2(d) = \gamma_s^d \sum_{i=0}^{d-1} \binom{d-1+i}{i} (1-\gamma_s)^i \quad (\text{A.5})$$

where  $\gamma_s = 0.5(1 - \sqrt{R_c \gamma_b / (1 + R_c \gamma_b)})$  and  $\gamma_b = E_b / N_o$  [43]. This probability is the d-th order time diversity, which is equivalent to the d-th order path diversity when the max ratio combining is applied.

### A.3.2 Union Upper Bound on BER of RS Codes

The union upper bound on PER can be constructed based on the symbol error rate, which is derived from the union bound on the BER of RCPC. A union upper bound on the PER of the RS code is expressed in the form

$$P_{p,RS} \leq \sum_{i=i_c+1}^n \binom{n}{i} p^i (1-p)^{n-i} \quad (\text{A.6})$$

where  $p = 1 - (1 - P_{b,RCPC})^{1/8}$ . When an RS code word error occurs, the associated 8-bit symbol error rate is given by

$$P_{s,RS} \leq \frac{1}{n} \sum_{i=i_c+1}^n i \binom{n}{i} p^i (1-p)^{n-i} \quad (\text{A.7})$$

and the corresponding upper bound on BER is approximated by

$$P_{b,RS} \leq \frac{2^{k-1}}{2^k - 1} P_{s,RS} \quad (\text{A.8})$$

## A.4 Simulation Results

In this section, the average BERs of RCPC and RS codes are calculated using the simulated data. The BER values are plotted and compared to the corresponding theoretical upper bounds for the code rates 1/2, 2/3, 3/4, 5/6, and 7/8. In the simulation, up to  $10^7$  data bits are transmitted. Simulations are plotted on Figs. A.2-5, where T and S denote theoretical bound and simulation results respectively. Simulation results of BER are close to the theoretical bounds, particularly when the signal-to-noise ratio is large. These results are consistent with

the findings of the previous study [43]. Also, it shows that simulation results and theoretical upper bounds are fairly tight. In addition, the uncoded BER curve is also plotted. It is clearly shown that the coding gain can be obtained if the signal-to-noise ratio is sufficiently large.

Fig. A.6-7 showed the average PER of 255-byte RS packets in the AWGN and FI-RFC channels, where A and R denote AWGN and FI-RFC channels respectively. With this data, researchers who are primarily interested in packet-based transmission might simulate their testing platform more easily with IEEE802.16a specification and get more realistic results.

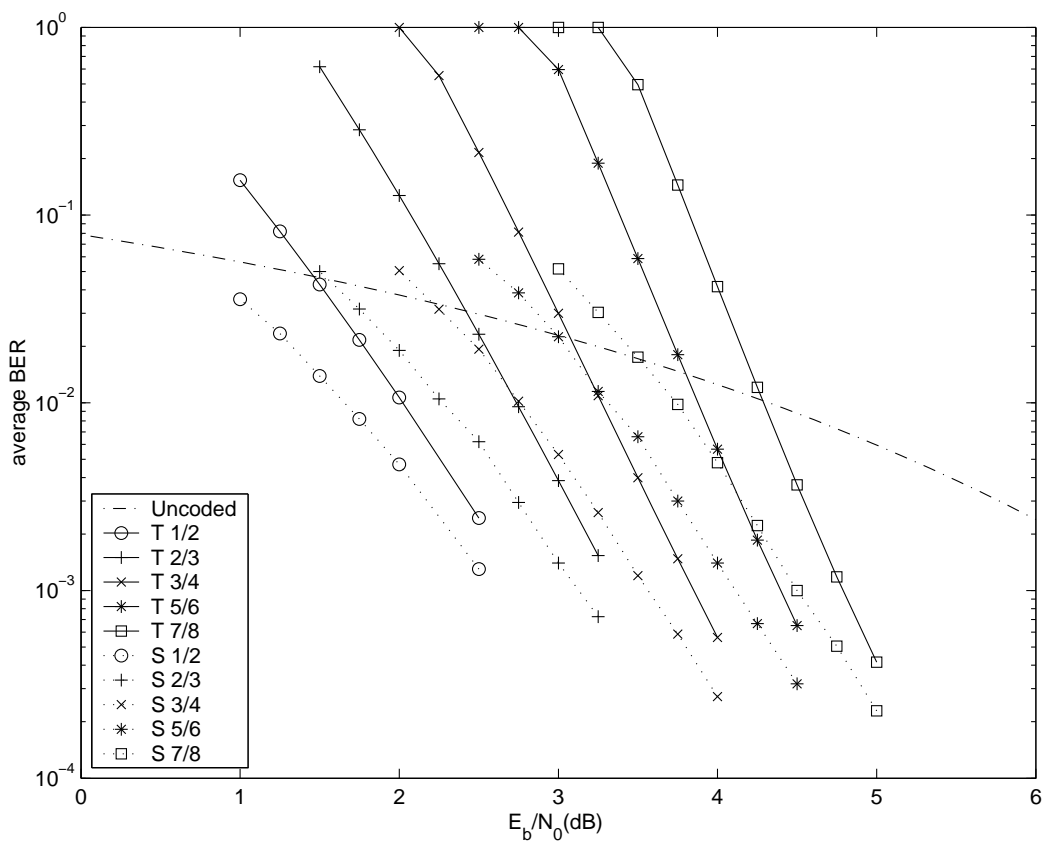


Fig. A.2. BER of RCPC codes in AWGN.

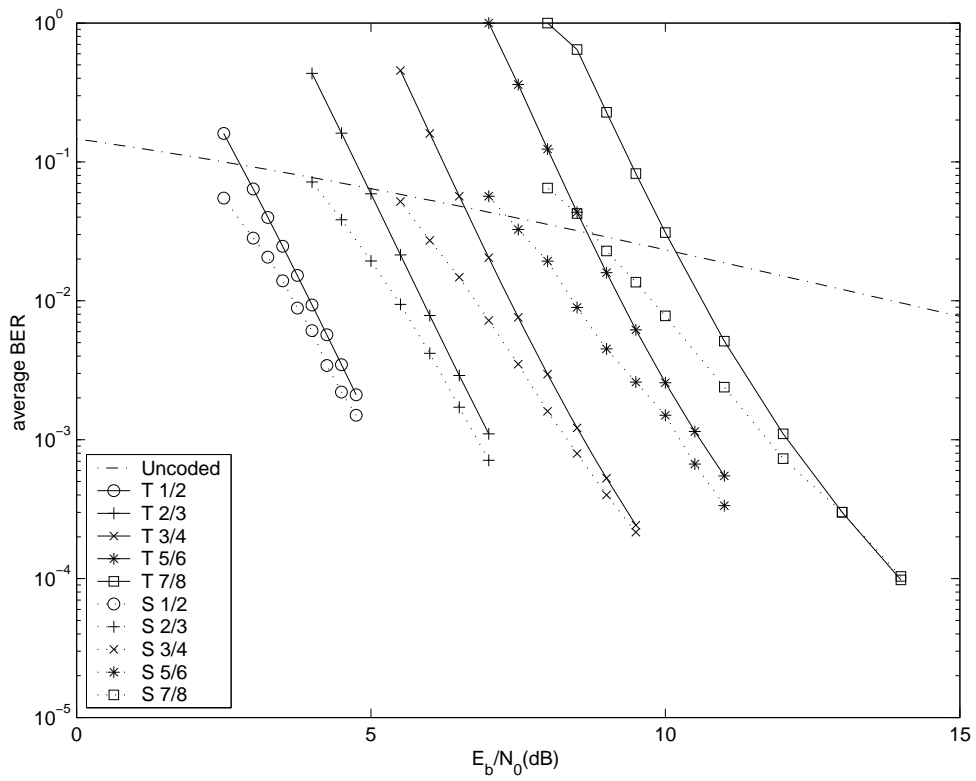


Fig. A.3. BER of RCPC codes in FI RFC.

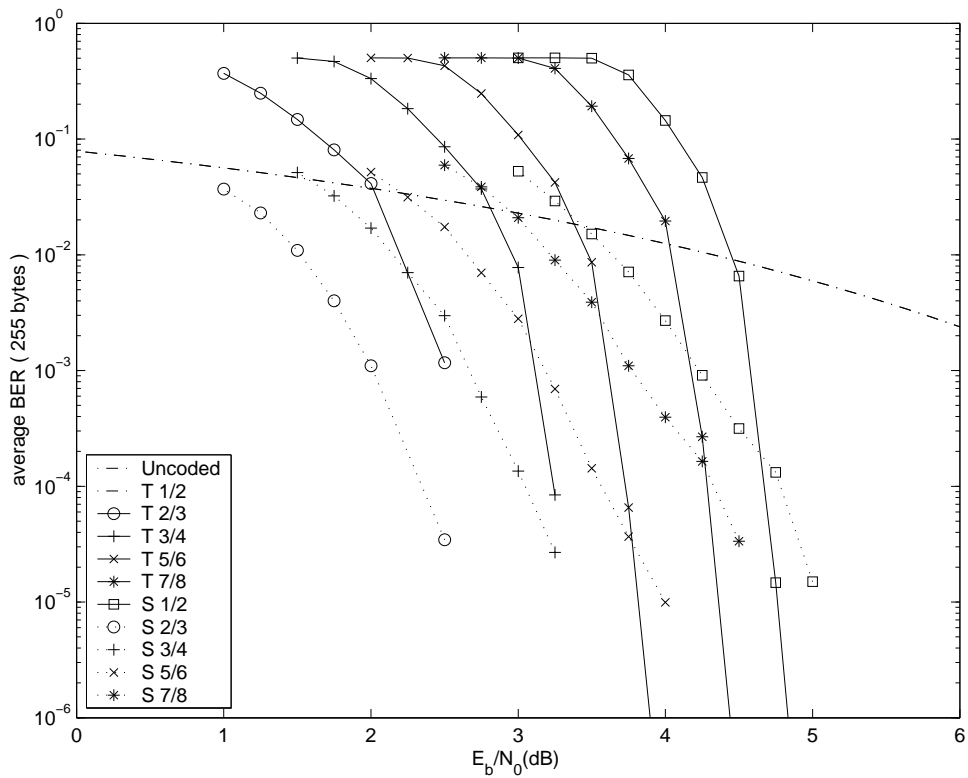


Fig. A.4. BER of RS code in AWGN.



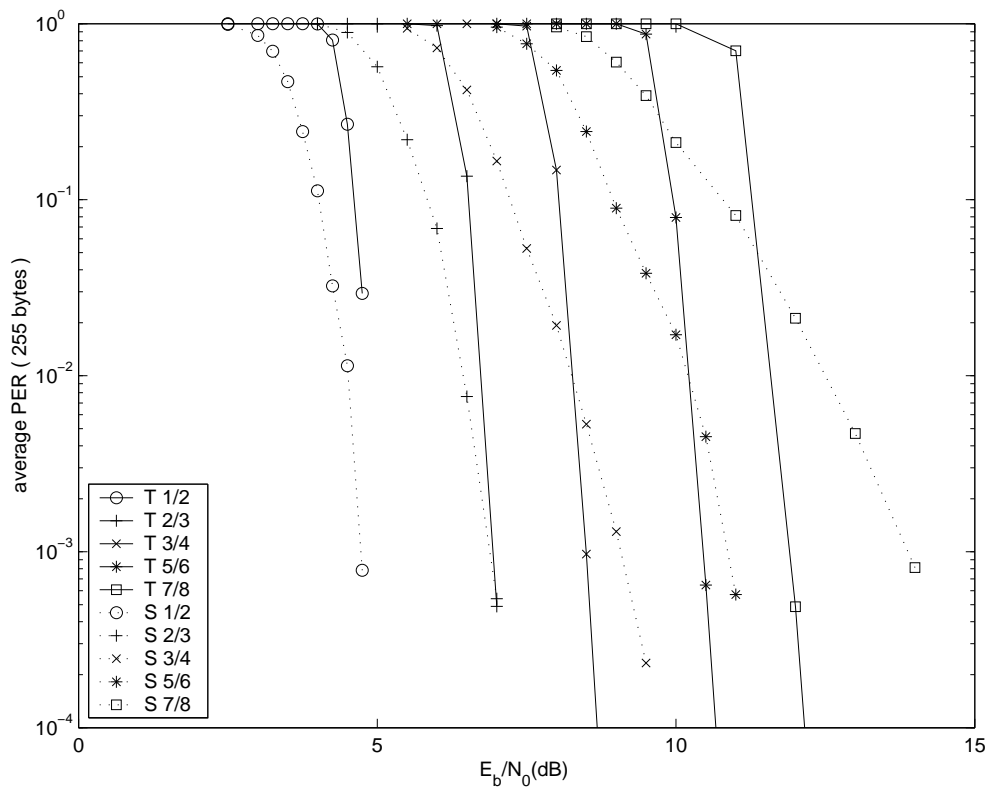


Fig. A.5. BER of RS code in FI-RFC.

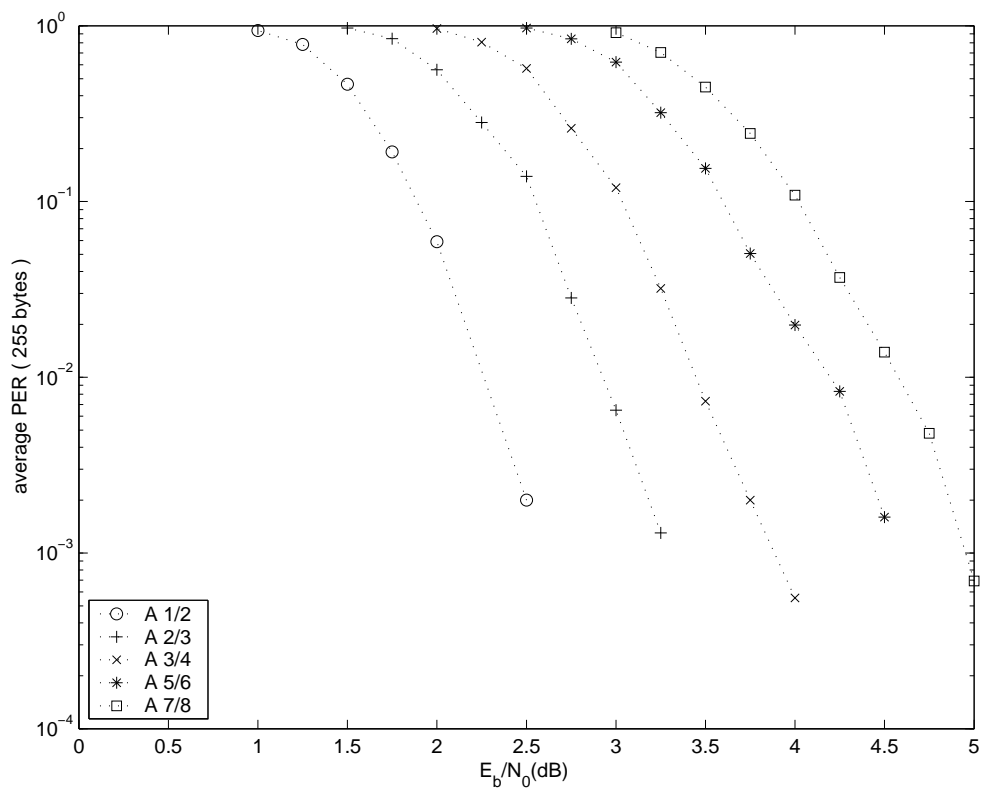


Fig. A.6. PER of RS code in AWGN.

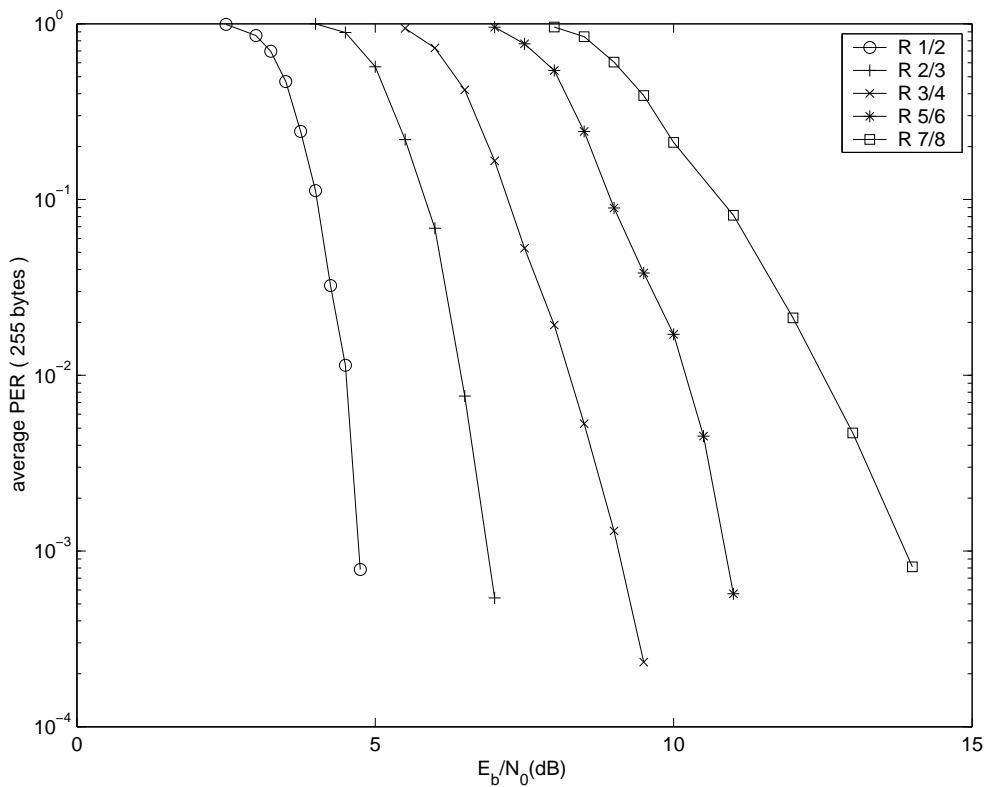


Fig. A.7. PER of RS code in FI-RFC.

## A.5 Conclusions

In this appendix, the performance of the serially concatenated CFEC defined by the IEEE802.16a specifications is analyzed and simulated for both AWGN and RFC channels. The RFC channel is assumed to be slow and flat fading and is fully interleaved. Moreover, the soft decision Viterbi decoding has no quantization. The upper bounds on BER of RCPC and RS codes have been derived and are compared to the simulation results. We thus found that the upper bounds are quite tight.

Also, the PER performance is simulated and summarized. With this set of data, researchers interested in packet-based transmission could easily design their IEEE802.16a systems that meet the target performance. In conclusion, we provide a suitable operational range for IEEE802.16a, which is a trade-off between the signal to noise ratio and the desired performance.

# Bibliography

- [1] ISO/IEC, *Information Technology-Coding of Moving Pictures and Associated Audio for Digital Storage Media at up to About 1.5 Mbit/s: Video*, ISO/IEC 11172-2(MPEG-1 Video), 1993.
- [2] ISO/IEC, *Information Technology-Generic Coding of Moving Pictures and Associated Audio Information: Video*, 13818-2-ITU-T Rec. H.262(MPEG-2 Video), 1995.
- [3] ISO/IEC, *Information Technology-Generic Coding of Audio-Visual Objects Part 2: Visual*, ISO/IEC 14496-2(MPEG-4 Video), 1999.
- [4] "Video coding for low bitrate communication," ITU-T Recommendation H.263 Version 1, 1995. Version 2, Sept. 1997.
- [5] T.Wiegand, G.-J. Sullivan, G. Bjontegarrd, and A. Luthra, "Draft ITU-T Rec. H.264/ISO/IEC 14496-10 AVC," Joint Video Team of ISO/IEC MPEG and ITU-T VCEG, Doc. JVT-G050r1, Mar. 2003.
- [6] Joint Video Team of ISO/IEC MPEG and ITU-T VCEG, "Joint Final Committee of Joint Video Specification (Draft ITU-T Rec. H.264/ ISO/IEC 14496-10 AVC)," Doc. JVT-D157, Aug. 2002.
- [7] T.Wiegand, G.-J. Sullivan, G. Bjontegarrd, and A. Luthra, "Overview of the H.264/AVC video coding standard," *IEEE Trans. Circuits Syst. Video Technol.*, vol. 13, pp. 560-576, Jul. 2003.
- [8] A.-E. Mohr, "Bit allocation in sub-linear time and the multiple-choice knapsack problem," in *Proc. IEEE. Data Compression Conf.*, pp. 352-361, Mar. 2002.
- [9] K. Ramchandran, A. Ortega, and M. Vetterli, "Bit allocation for dependent quantization with application to multi-resolution and MPEG video coders," *IEEE Trans. Image Processing*, vol. 3, no. 5, pp. 533-545, Sep. 1994.

- [10] Y. Sermadevi and S.-S. Hemami, "Efficient bit allocation for dependent video coding," in *Proc. IEEE. Data Compression Conf.*, pp. 232-241, Mar. 2004.
- [11] A. Ortega, K. Ramchandran, and M. Vetterli, "Optimal trellis-based buffered compression and fast approximations," *IEEE Trans. Image Processing*, vol. 3, pp. 26-40, Jan. 1994.
- [12] A. Ortega and K. Ramchandran, "Rate-distortion methods for image and video compression," *IEEE Signal Processing Magazine*, Nov., 1998.
- [13] H.-M. Hang and J.-J. Chen, "Source model for video transform coder and its application – part I: fundamental theory," *IEEE Trans. Circuits Syst. Video Technol.*, vol. 7, pp. 287-298, Apr. 1997.
- [14] J.-J. Chen and H.-M. Hang, "Source model for video transform coder and its application – part II: variable frame rate coding," *IEEE Trans. Circuits Syst. Video Technol.*, vol. 7, pp. 299-311, Apr. 1997.
- [15] T. Chiang and Y.-Q. Zhang, "A new rate control scheme using quadratic rate distortion model," *IEEE Trans. Circuit Syst. Video Technol.*, vol. 7, pp. 246-250, Feb. 1997.
- [16] Z. He and S.-K. Mitra, "A unified rate-distortion analysis framework for transform coding," *IEEE Trans. Circuit Syst. Video Technol.*, vol. 11, pp. 1221-1236, Dec. 2001.
- [17] L.-J. Lin and A. Ortega, "Bit-rate control using piecewise approximated rate-distortion characteristics," *IEEE Trans. Circuit Syst. Video Technol.*, vol. 8, pp. 446-459, Aug. 1998.
- [18] G.-M. Schuster, G. Melnikov, and A.-K. Katsaggelos, "A overview of the minimum maximum criterion for optimal bit allocation among dependent quantizers," *IEEE Trans. Multimedia*, vol. 1, pp. 3-17, Mar. 1999.
- [19] Y. Shoham, and A. Gersho, "Efficient bit allocation for an arbitrary set of quantizers," *IEEE Trans. Acoustics, Speech and Signal Processing*, vol. 36, no. 9, pp. 1445-1453, Sep. 1988.

- [20] J. Ribas-Corbera and S. Lei, "Rate control in DCT video coding for low-delay communications," *IEEE Trans. Circuits Syst. Video Technol.*, vol. 9, no. 1, pp. 172-185, Feb. 1999.
- [21] Z. He and S.-K. Mitra, "Optimum bit allocation and accurate rate control for video coding via  $\rho$ -domain source modeling," *IEEE Trans. Circuit Syst. Video Technol.*, vol. 12, pp. 840-849, Oct. 2002.
- [22] D.-K. Kwon, M.-Y. Shen, and C.-C. Jay Kuo, "Rate control for H.264 video with enhanced rate and distortion models," *IEEE Trans. Circuit Syst. Video Technol.*, vol. 17, no. 5, pp. 517-529, May 2007.
- [23] Y. Yu, J. Zhou, Y. Wang, and C.-W Chen, "A novel two-pass VBR coding algorithm for fixed-size storage application," *IEEE Trans. Circuit Syst. Video Technol.*, vol. 11, no. 3, pp. 345-356, Mar. 2001.
- [24] Z. He, W. Zeng, and C.-W Chen, "Low-Pass filtering of rate-distortion functions for quality smoothing in real-time video communication," *IEEE Trans. Circuit Syst. Video Technol.*, vol. 15, no. 8 pp. 973-981, Aug. 2005.
- [25] B. Xie, and W. Zeng, "A sequence-based rate control framework for consistent quality real-time video," *IEEE Trans. Circuit Syst. Video Technol.*, vol. 11, no. 3, pp. 56-71, Jan. 2006.
- [26] Y. Sermadevi and S.-S. Hemami, "Lexicographic bit allocation for MPEG video coding," in *Proc. IEEE. Data Compression Conf.*, pp. 101-110, Mar. 1997.
- [27] N. Cherniavsky, et al., "MultiStage: a MINMAX bit allocation algorithm for video coders," *IEEE Trans. Circuit Syst. Video Technol.*, vol. 17, no. 1, pp. 59-67, Jan. 2007.
- [28] S.-Y. Lee and A. Ortega, "Optimal rate control for video transmission over VBR channels based on a hybrid MMAX/MMSE criterion," in *Proc. IEEE Int. Conf. Multimedia Expo*, vol. 2, pp. 93-96, Aug. 2002.

- [29] G.-D. Forney, "The Viterbi algorithm," in *Proc. IEEE.*, vol. 1 ,no. 61, pp. 268-278, Mar. 1973.
- [30] W.-Y. Lee and J.-B. Ra, "Fast algorithm for optimal bit allocation in a rate-distortion sense," in *Electronics Letters*, vol. 32, no. 20, pp. 1871-1873, Sep. 1996.
- [31] C.E. Shannon, "A mathematical theory of communication," *Bell Syst. Tech. Journal*, vol. 27, pp. 379-423, 1948.
- [32] C.E.Shannon, "Coding theorems for a discrete source with a fidelity criterion," in *IRE National Convention Record*, Part 4, pp. 142-163, 1959.
- [33] T.Berger, *Rate-Distortion Theory. A Mathematical Theory for Data Compression.* Prentice-Hall, 1971.
- [34] A.-R. Reibman and B.-G. Haskell, "Constraints on variable bit-rate video for ATM networks," *IEEE Trans. Circuit Syst. Video Technol.*, vol. 2, pp. 361-372, Dec. 1992.
- [35] J.-J. Chen and D.W. Lin, "Optimal bit allocation for coding of video signals over ATM networks," *IEEE J. Selected Areas in Communication.*, vol. 3, pp. 1002-1015, Aug. 1997.
- [36] K.-L. Huang and H.-M. Hang, "Consistent picture quality control strategy for dependent video coding," *IEEE Trans. Image Processing*, vol. 18, no. 5, pp. 1004-1014, May 2009.
- [37] J.Hagenauer, "Rate-compatible punctured convolutional codes (RCPC Codes) and their applications," *IEEE Trans. Communications*, vol. 36, no. 4, pp. 389-400, Apr. 1988.
- [38] K.-L. Huang and H.-M. Hang, "Performance analysis for serially concatenated FEC in IEEE802.16a over wireless channels," *5th Pacific Rim Conference on Multimedia*, pp. 672-679, Dec. 2004.
- [39] IEEE Std. 802.16-2004, "IEEE standard for local and metropolitan area networks – part 16: air interface for fixed broadband wireless access systems," Oct. 2004.
- [40] G. Solomon and H. C. A. van Tilborg, "A connection between block and convolutional codes," *Slam J. Appl. Mathematics*, vol. 37, no. 2, pp. 358-369, Oct. 1979.

- [41] J.Hagenauer, "Viterbi decoding of convolutional codes for fading- and burst-channels," in *Proc. Int. Seminar Digital Commun., Zurich, Switzerland*, pp. G2.1-G2.7, Mar. 1980.
- [42] G. Begin, D.Haccoun, and C. Paquin, "Further results on high-rate punctured convolutional codes for Viterbi and sequential decoding," *IEEE Trans. Communications*, vol. 38, no. 11, pp. 1922-1928, Nov. 1990.
- [43] J. G. Proakis, *Digital Communication*, 3<sup>rd</sup> ed. New York, McGraw-Hill, 1995.



# 簡歷

姓 名：黃國隆

性 別：男

籍 貫：上海市

出生地：台灣、台北

學歷：

中正理工學院電機工程系學士 西元 1981 年 9 月 ~ 1985 年 6 月

中正理工學院電子工程研究所碩士 西元 1987 年 9 月 ~ 1989 年 6 月

國立交通大學電子研究所博士班 西元 2000 年 9 月入學

經歷：

中正理工學院電機工程系助教 西元 1985 年 7 月 ~ 1987 年 6 月

中山科學研究院第三研究所 西元 1989 年 7 月 ~ 2000 年 8 月

中山科學研究院電子系統研究所 西元 2004 年 9 月 ~

博士論文：

用於相依視訊編碼之影質控制策略

Picture Quality Control Strategies for Dependent Video Coding